Bull Volcanol (2003) 65:363–381
DOI 10.1007/s00445-003-0277-y

RESEARCH ARTICLE

A. Mark Jellinek · Donald J. DePaolo

A model for the origin of large silicic magma chambers: precursors of caldera-forming eruptions

Received: 4 June 2002 / Accepted: 13 January 2003 / Published online: 6 May 2003

Abstract The relatively low rates of magma production in island arcs and continental extensional settings require that the volume of silicic magma involved in large catastrophic caldera-forming (CCF) eruptions must accumulate over periods of 10^5 to 10^6 years. We address the question of why buoyant and otherwise eruptible high-silica magma should accumulate for long times in shallow chambers rather than erupt more continuously as magma is supplied from greater depths. Our hypothesis is that the viscoelastic behavior of magma chamber wall rocks may prevent an accumulation of overpressure sufficient to generate rhyolite dikes that can propagate to the surface and cause an eruption. The critical overpressure required for eruption is based on the model of Rubin (1995a). An approximate analytical model is used to evaluate the controls on magma overpressure for a continuously or episodically replenished spherical magma chamber contained in wall rocks with a Maxwell viscoelastic rheology. The governing parameters are the long-term magma supply, the magma chamber volume, and the effective viscosity of the wall rocks. The long-term magma supply, a parameter that is not typically incorporated into dike formation models, can be constrained from observations and melt generation models. For effective wall-rock viscosities in the range 10^{18} to 10^{20} Pa s^{-1}, dynamical regimes are identified that lead to the suppression of dikes capable of propagating to the surface. Frequent small eruptions that relieve magma chamber overpressure are favored when the chamber volume is small relative to the magma supply and when the wall rocks are cool. Magma storage, leading to conditions suitable for a CCF eruption, is favored for larger magma chambers (>10^2 km^3) with warm wall rocks that have a low effective viscosity. Magma storage is further enhanced by regional tectonic extension, high magma crystal contents, and if the effective wall-rock viscosity is lowered by microfracturing, fluid infiltration, or metamorphic reactions. The long-term magma supply rate and chamber volume are important controls on eruption frequency for all magma chamber sizes. The model can explain certain aspects of the frequency, volume, and spatial distribution of small-volume silicic eruptions in caldera systems, and helps account for the large size of granitic plutons, their association with extensional settings and high thermal gradients, and the fact that they usually post-date associated volcanic deposits.

Keywords Dike Formation · Viscoelastic Rocks · Rhyolitic Volcanism · Granitic Plutons · Silicic Magma Chumber Evolution

Editorial responsibility: T.H. Druitt

A. M. Jellinek (✉)
Department of Physics,
University of Toronto,
Toronto, Canada M5S 1A7
e-mail: markj@seismo.berkeley.edu

D. J. DePaolo
Department of Earth and Planetary Science,
University of California,
Berkeley, CA 94720-4767, USA

D. J. DePaolo
Earth Sciences Division,
E.O. Lawrence Berkeley National Laboratory,
Berkeley, CA 94720, USA

Introduction

One of the most impressive of the volcanic phenomena documented in the geologic record are cataclysmic caldera-forming (CCF) eruptions (Smith 1979). In a single such event, lasting from days to weeks, as much as 2,000 km^3 (some estimates reach 5,000 km^3) of magma can be erupted. By comparison, the magma output from all of the active Hawaiian volcanoes, which constitute the most intense basaltic volcanism on Earth, is about 0.15 km^3 $year^{-1}$ (Lipman 1995). The largest CCF eruptions are explosive, involve silica-rich magma (Hildreth 1981), and are fed by shallow (5–10-km depth) magma chambers located in regions of thick continental crust. Many of the volcanic systems that produce CCF

eruptions are associated with subduction, although regional extension seems to be an important and common feature as well (Wood 1984; Lipman 2000). There are several candidate areas for further large CCF eruptions in the western United States, such as Yellowstone, Long Valley, California, and the Jemez Mountains, New Mexico. Other candidate areas include, for example, the Taupo volcanic zone in New Zealand (e.g., Wilson et al. 1995; Jurado-Chichay and Walker 2001a, 2001b), volcanic regions in Kamchatka (e.g., Bratseva et al. 1996), the Philippines (Punongbayan et al. 1991; Simkin 1993), and the Andes (Pritchard and Simons 2002). A better understanding of the conditions necessary for large CCF eruptions is desirable because an improved ability to specify the likelihood of such eruptions would figure prominently in the assessment of volcanic hazards associated with silicic caldera systems (e.g., Simkin 1993; Newhall et al. 1994; Pyle 1998; Denlinger and Hoblitt 1999; McNutt 2000).

In this paper, we address a fundamental issue raised by the large volumes of CCF eruptions, which is how buoyant magma can accumulate in the upper crust rather than be erupted at about the rate magma is supplied from deeper levels. From the existence of large granitic batholiths it is clear that accumulations of thousands of cubic kilometers of high-silica, low density magma in the upper crust is a common occurrence. Although the accumulation of magma may be explained if the crystal content is sufficiently high to prevent eruption (e.g., Marsh 1988), the phenomenon of accumulation of buoyant, eruptible magma in the upper crust has gone without explanation.

Our approach to this problem focuses on the dynamical requirements for rhyolite dikes to form at the walls of a crustal magma chamber and propagate to the surface, resulting in an eruption (Rubin 1995a). The Rubin (1995a) model predicts that the leading tip of a rhyolite dike will freeze, arresting dike propagation, unless the pressure driving the flow of magma in the dike is of a sufficiently large magnitude. This model produces estimates of the critical magma chamber overpressure for rhyolite dikes in the range of 10–40 MPa, which is about one order of magnitude higher than the overpressure needed to cause the crack tip intensity factor to exceed the fracture toughness of most rocks (Rubin 1995b; McLeod and Tait 1999). We argue that if the wall rocks behave as Maxwell viscoelastic rather than purely elastic solids, and if the effective viscosity of the wall rocks is sufficiently low, conditions exist in which it can be difficult or impossible to erupt high-silica magmas because dikes cannot propagate from the chamber to the surface without freezing. We show that whether magma erupts or accumulates in an expanding chamber, depends on the temperature and strain rate in the bounding wall rocks, the latter being determined by the ratio of the magma supply to the chamber volume and, to a lesser extent, tectonic regime. Moreover, this model can explain how the large silicic magma reservoirs needed for voluminous CCF eruptions can be maintained in the mid- to upper crust for long periods, given that the supply of new magma is sufficient to outpace crystallization. Finally, our model yields a potential explanation for the recurrence interval of smaller volume (0.1–10 km^3) eruptions, which typically also occur in caldera systems.

Magma supply for large eruptions

The motivation for our model is that the large volumes of CCF eruptions require that magma be accumulated and stored in shallow crustal reservoirs for long periods of time prior to eruption. To appreciate this point, it is necessary to consider the rates at which both mafic and silicic magmas are produced in the subduction zone and extensional environments in which most silicic volcanism occurs. Assuming that each volcano in an arc captures magma from a 50- to 100-km length of arc, which is a typical volcano spacing (Marsh and Carmichael 1974; Schimozuro and Kubo 1983; Tatsumi and Eggins 1995), models of magma production rates in subduction zones suggest values of about 0.001 to 0.01 $km^3\ year^{-1}$ per volcano (cf. Davies and Bickle 1991). This range is higher than the long-term accretion rate of arc volcanic rocks, which is estimated to be 17 to 33 km^3 million $years^{-1}\ km^{-1}$ of arc, or 0.00085 to 0.0034 $km^3\ year^{-1}$ per volcano assuming the same 50 to 100 km volcano spacing (Brown and Mussett 1981; Reymer and Schubert 1984). Studies of the growth rates of individual stratovolcanoes suggest somewhat lower rates of 0.0001 to 0.001 $km^3\ year^{-1}$ (Davidson and DeSilva 2000).

For comparison, this range of fluxes is one to three orders of magnitude smaller than the supply of magma at Hawaii (0.15 $km^3\ year^{-1}$ distributed between three volcanoes), but substantially greater than the magma supply at continental extensional environments uninfluenced by hotspot volcanism. For example, in the Basin and Range of the southwestern United States, the average eruption rate of basalt during the past 16 million years, normalized to the area of a typical volcanic system (about $10^3\ km^2$), is only 10^{-5} to $10^{-7}\ km^3\ year^{-1}$ (Crowe 1986).

The magma produced in subduction zones is expected to have the composition of basalt or basaltic andesite (48–54% SiO_2; Green 1973; Davies and Bickle 1991). One way to produce rhyolite from such magma is by extensive (70–90%) fractional crystallization, which implies that the supply of rhyolite in subduction zone settings is three to ten times smaller than the total magma supply values cited above. However, almost all of the large-volume CCF eruptions documented in the literature contain a sizeable proportion of magma (or assimilated rock material) derived from the crust. Hence, it appears that in regions of thick continental crust, crustal melting and assimilation augment the rhyolite magma supply. On the basis of isotopic data and thermal balance models, the crustal contribution to the magma flux appears typically to be two to ten times the magma supply due to subduction alone (Johnson 1991; DePaolo et al. 1992; Perry et al. 1993). Consequently, the supply of rhyolite to

a continental volcanic system in a region of thick continental crust can be expected to be as high as 0.001 to 0.005 km^3 $year^{-1}$. Insofar as documented storage rates of high silica magma are in this range (e.g., Spera and Crisp 1981), and that fractional crystallization is likely to be involved, the flux of more mafic magma into the high level system could be closer to 0.01 km^3 $year^{-1}$.

These values for average silicic magma fluxes are in agreement with those calculated on the basis of eruption volumes and repose times in systems in which there have been recurrent CCF eruptions. Well-studied examples include the Valles and Yellowstone calderas (Smith 1979; Christiansen 1984) and the Okataina volcanic center, Taupo, New Zealand (e.g., Bailey 1965; Davis 1985; Bailey and Carr 1994; Schmitz 1995; Jurado-Chichay and Walker 2001a, 2001b). The range of silicic magma supply also brackets the canonical value of 0.002 km^3 $year^{-1}$ used by Smith (1979). Direct geophysical measurements also yield comparable magma fluxes on relatively short time scales. Whereas the volumetric inflation rate at Long Valley between 1979 and 1998 has been estimated to be about 0.006–0.02 km^3 $year^{-1}$ (Hill et al. 1985; Battaglia et al. 1999), the inferred inflation rate for the Socorro magma body is around 0.006 km^3 $year^{-1}$ (Fialko et al. 2001). Thus, to accumulate enough silicic magma for an eruption of 1,000 km^3 or more takes 10^5 to 10^6 years.

That large silicic magma bodies accumulate continuously over time through injections of both mafic and silicic magma is also supported by studies of large granitic plutons, which may be associated with silicic volcanic rocks (e.g., Wiebe 1974, 1993, 1994, 1996; Michael 1991; Snyder and Tait 1995, 1996; Wiebe and Collins 1998; Wiebe et al. 2002). The issue of magma supply was apparently circumvented by Huppert and Sparks (1988) in their model of the rapid production of large quantities of silicic magma by wholesale melting of preheated crustal rocks immediately overlying basaltic sills. However, although instructive the Huppert and Sparks (1988) model is misleading with regard to CCF systems in two ways. First, CCF systems erupt silicic magma that is largely derived by fractional crystallization of more mafic magma (Johnson 1991; DePaolo et al. 1992; Perry et al. 1993), albeit with concurrent assimilation. Second, the model does not account for the time required to produce the basalt for the sill. Since these authors calculate a roughly 1:1 ratio of basalt and silicic magma, an implication is that it takes the same amount of time to produce the basalt for the sill in a subduction zone environment (i.e., 10^5–10^6 years) as we calculate to accumulate silicic magma. This result is, however, inconsistent with results from high-precision geochronological studies of active volcanic systems. Evidence from short-lived U-series isotopes suggests that, for example, basalt is seldom stored longer than about 10^3 years before being erupted or injected into a shallow magma chamber (e.g., Cohen and O'Nions 1993; Hemond et al. 1994; Sims et al. 1999).

Thermal survival of dikes and wall-rock rheology

Dike propagation is generally thought to result from an influx of magma that causes the pressure in a chamber to rise over that of the surrounding rocks in response to the expansion of the chamber walls (e.g., Blake 1984; Tait et al. 1989; McLeod and Tait 1999). If a dike propagates to the Earth's surface (Spence and Turcotte 1985; Lister and Kerr 1991; Rubin 1995b; Meriaux and Jaupart 1995, 1998), typically a distance of 5 to 10 km, a volcanic eruption can result (Wilson et al. 1980).

Models of dike formation commonly treat the wall rocks as homogeneous, purely elastic, isotropic media with a constant strength and material stiffness, and neglect effects such as the temperature- and strain rate-dependence of wall-rock rheology, the magma supply, and the shape and size of a magma chamber (e.g., Blake 1984; Tait et al. 1989; McLeod and Tait 1999). A fixed flux of magma into a spherical chamber bounded by perfectly elastic wall rocks produces a stress increase in the wall rocks at a rate proportional to the fractional increase in chamber volume (this concept is developed further below). If the influx persists, the magma pressure required to generate a dike will inevitably be reached. However, if the wall rocks are sufficiently warm and the strain rates due to chamber growth are appropriate, the effective viscosity of the wall rocks may be low enough such that the chamber overpressure drives radial creep (effectively viscous flow) in the wall rocks, which can, in turn, limit the maximum sustainable magma overpressure. For the model and discussion that follows it will be useful to introduce the "flow stress" of the wall rocks (cf. Carter and Tsenn 1987), which is the viscous stress corresponding to the radial strain rate arising due to chamber expansion. The flow stress depends on temperature, radial strain rate, and the bulk composition of the wall rocks.

The magma chamber overpressure, $\triangle P_{ch}$, needed to form a dike of length ℓ is thought to be only a few MPa, which is also approximately the pressure needed for the crack-tip stress intensity factor K (e.g., Griffith 1920; Anderson 1995; Rubin 1995a; McLeod and Tait 1999),

$$K = 1.12\Delta P_{ch}(\ell)^{1/2} \quad (1)$$

to exceed the fracture toughness, K_c, of crustal rocks (Rubin 1995b). We note that this overpressure reflects the criterion for an existing magma-filled crack in the chamber wall to propagate into the wall rock. In contrast, the overpressure required to nucleate a new fracture in the chamber wall is much larger, closer to 50 MPa (e.g., Rubin 1995b).

Rubin (1995a) argues that the criterion $K>K_c$ is insufficient to insure that a dike will propagate to the surface. If the dike is propagating into rocks of progressively lower temperature, as would be the case for a dike leaving a magma chamber, the flow rate of magma into the propagating dike must be sufficiently large that the dike widens faster than it narrows as a result of freezing at the walls (see also Lister and Kerr 1991; Petford et al.

1993; 1994). Rubin (1995a) shows that the criterion for the thermal survival of dikes can be expressed in terms of a dimensionless parameter, β:

$$\beta = 2\left(\frac{3\kappa\mu_m}{\pi\Delta P_{ch}}\right)^{1/2} c|dT_{wr}/dx| \frac{L}{E}\left(\frac{\Delta P_{ch}}{E}\right)^{-2} \quad (2)$$

where κ, c, and μ_m are the thermal diffusivity, specific heat and viscosity of the magma, dT_{wr}/dx is the temperature gradient in the wall rocks along the path of the dike and E is the elastic modulus of the wall rocks. In all calculations that follow we take E=10^{10} Pa, which is about two to five times smaller than laboratory measured values, but thought to be appropriate for crustal rocks (e.g., Bienawski 1984; Rubin 1995a, 1995b). Assuming the magma has a constant average viscosity and a eutectic composition numerical models indicate that dikes cannot propagate unless β is less than about 0.12 to 0.16, depending on the relative magnitudes of the pressures in the chamber, in the dike and in the (magma-free) propagating dike tip. This range for β is conservative. In particular, vertical and lateral temperature variations in the magma within the dike, combined with volatile exsolution into the wall rocks, could lead to large increases in magma viscosity near the walls and the dike tip, which would inhibit magma flow and, thus, enhance the retarding effect of solidification on dike propagation. Nevertheless, the major result of this model is that low viscosity basaltic dikes are much more likely to propagate through cold wall rocks to the surface than high viscosity rhyolitic dikes.

By setting β to a nominal value of 0.15 in Eq. (2), we can rearrange to get an expression for the critical overpressure, $\triangle P_{\rm crit}$, needed to propagate a dike to the surface to generate an eruption:

$$\Delta P_{crit} = 3.5\left[\left(\frac{\kappa\mu_m}{\pi}\right)^{1/2} c|dT_{wr}/dx| \frac{L}{E^2}\right]^{2/5} \quad (3)$$

where the numerical constants on the right-hand side have been combined and rounded off. Figure 1a, b gives $\triangle P_{\rm crit}$ as a function of magma viscosity for different values of the temperature gradient. The temperature gradients chosen correspond to heat flow values of 0.2 to 0.8 W m^{-2}, a range consistent with surface heat fluxes measured in geothermal areas (e.g., Palmaesson and Saemundson 1974; Fournier and Pitt 1985; Bibby et al. 1995). For typical rhyolite viscosities (10^5 to 10^7 Pa s^{-1}), the critical overpressure for dikes to propagate to the surface is roughly 10 to 40 MPa. This requirement also leads to the prediction that rhyolite dikes should be wider than basalt dikes, which is broadly consistent with observations (Lister and Kerr 1991; Rubin 1995a).

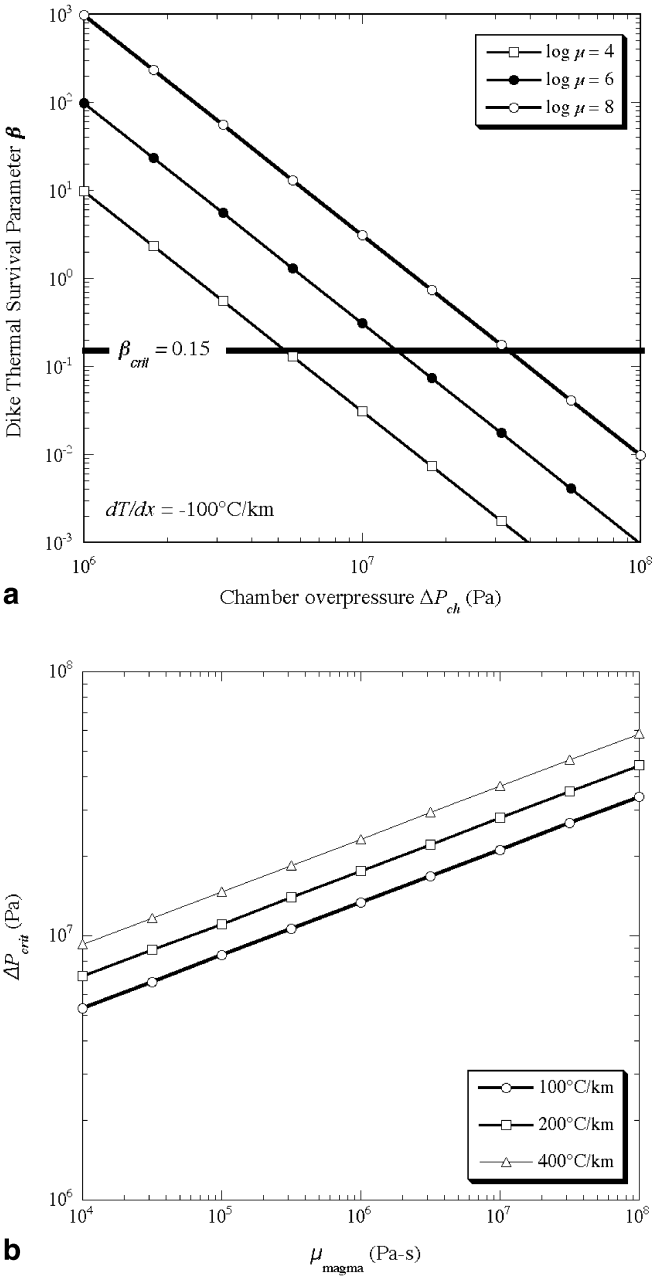

Fig. 1 **a** Variation of the dike thermal survival parameter β (cf. Rubin 1995a) as a function of chamber overpressure for different magma viscosities when the temperature gradient from the magma to the wall rocks is conservatively set to –100 °C km^{-1}. For a given nominal β=0.15, say, a much larger (critical) overpressure is required to propagate a high viscosity rhyolite dike to the surface than to propagate a low viscosity basalt dikes to the surface. **b** For a given β =0.15, the critical overpressure increases with both magma viscosity and the magnitude of the downstream temperature gradient

Summary of model components

Our approach has three main features. First, we assume a spherical magma-chamber shape. This allows us to calculate the stresses and strain rates resulting from an influx of new magma in a straightforward way. Second, we use the constraints on magma supply discussed above to govern the range of stresses and strain rates that are likely to characterize the growth of a magma chamber. Third, it will be shown that Maxwell viscoelastic behavior

in the wall rocks introduces an additional time scale and, hence, we use an extension of the dike nucleation model of McLeod and Tait (1999) to evaluate whether magma viscosity plays a role in setting the time scale for dike formation at the walls of a magma chamber. Using available observational and experimental data on the rheology of common crustal rocks (e.g., Kirby 1985; Carter and Tsenn 1987), the model is applied to first identify conditions leading to the suppression of rhyolite dikes that propagate to the surface and, thus, to the long-term accumulation and storage of silicic magma. Next, we evaluate the potential controls on the frequency of rhyolite eruptions under the conditions where rhyolite dikes are produced readily. The additional influences of regional tectonic stresses, unsteady or episodic magma influxes, crystallization, and magma buoyancy on dike formation are explored briefly, in turn.

Magma chamber and dike pressurization with viscoelastic wall rocks

Magma chamber pressurization

Our model spherical magma chamber is assumed to be embedded in a half-space with a Maxwell viscoelastic rheology (see also Bonafede et al. 1986; Dragoni and Magnanensi 1989; Anderson 1995; Newman et al. 2001), and supplied with new magma at a volumetric flow rate $Q(t)$ (Fig. 2). The pressure within the chamber, P_{ch}, is taken to be hydrostatic and the (radial) normal stresses on the chamber walls are uniaxial. The ambient stress field far from the magma chamber is assumed to be lithostatic. An influx of new magma causes the chamber to expand against the restoring force imposed by the wall rocks (which is governed by their rheology), resulting in an increase in P_{ch} above the normal values, which are set by the depth to the chamber and the buoyancy of the magma (Fig. 2). To a first approximation, this overpressure is $\triangle P_{ch} = P_{ch} - \sigma_r$, where σ_r is the remote lithostatic pressure (buoyancy is discussed separately in a later section).

Following the approach of Dragoni and Magnanensi (1989), the equation for a pressurized, expanding spherical chamber in an incompressible Maxwell viscoelastic half-space with a free upper surface can be written as:

$$\frac{2}{R_{ch}}\frac{dR_{ch}}{dt} = \frac{1}{E}\frac{d\Delta P_{ch}}{dt} + \frac{\Delta P_{ch}}{\mu_{wr}}, \quad (4)$$

where R_{ch} is the radius of the chamber and the effective viscosity, μ_{wr}, and elastic modulus, E, are taken to be

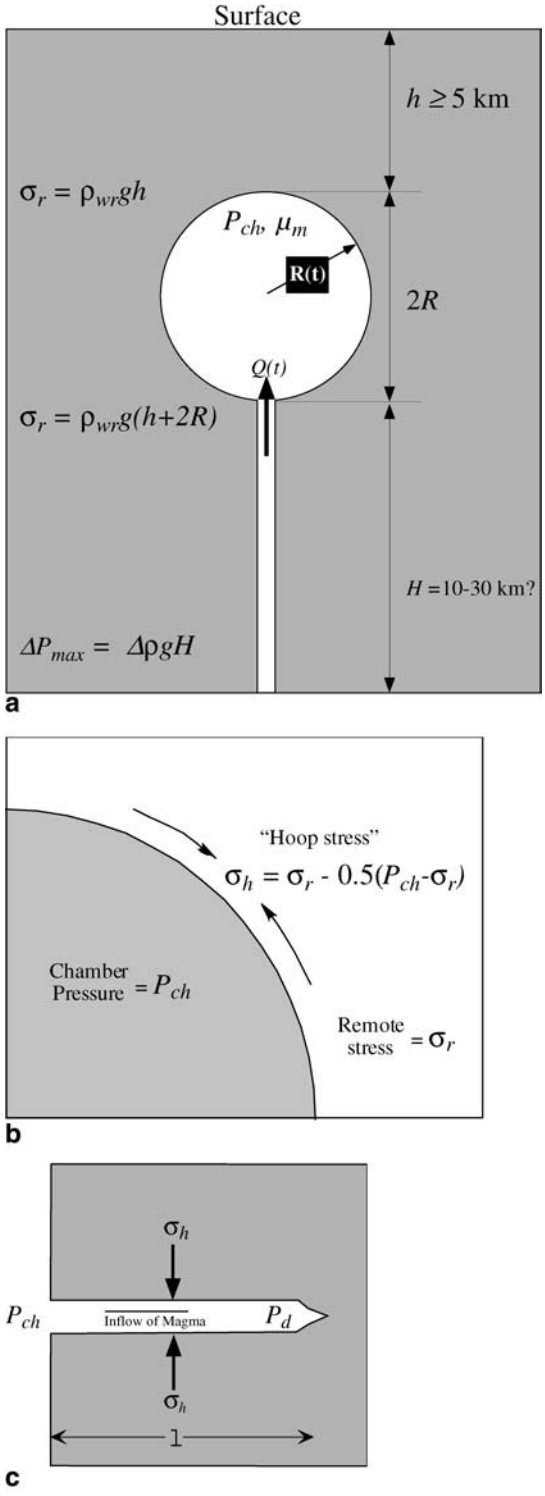

Fig. 2a–c Definition sketches for the dike nucleation problem. **a** The replenishment of a spherical magma chamber embedded in a crustal half space with a Maxwell viscoelastic rheology. A flux of new magma, which may be constant or variable in time, produces overpressure in the chamber that can lead, in turn, to dike formation. The maximum overpressure is determined by the height of the magma column underlying the magma chamber. **b** Definition of the chamber pressure, the remote stress and the "hoop stress", which is the stress parallel to the magma–wall rock interface. **c** Schematic illustration of a magma-filled crack and dike tip. The difference between the magma and dike pressures drives flow into the crack, which causes the pressure in the dike to rise. If the resultant stress concentration at the crack tip, is sufficiently large the crack will propagate into the wall rocks. In order for the dike to propagate to the surface and cause an eruption, however, the magma flux in the crack must exceed the rate of solidification (see text for discussion)

constant. The left-hand side of the equation is the radial strain rate in the wall rocks at the chamber wall. The right-hand side shows the elastic and viscous contributions to the strain rate, respectively (e.g., Dragoni and Magnanensi 1989). The pressure $\triangle P_{ch}$ is equal to the compressive deviatoric normal stress on the wall rocks at the chamber wall. Tangential to the chamber walls there is a tensile deviatoric stress equal to $-\triangle P_{ch}/2$ (Sammis and Julian 1987; Dragoni and Magnanensi 1989), so that the total stress, or "hoop stress" parallel to the chamber walls is:

$$\sigma_h(R_{ch}) = \sigma_r - \frac{\Delta P_{ch}}{2}. \quad (5)$$

For both elastic and viscoelastic wall rocks, the strain rates and the deviatoric stresses decrease with distance from the chamber as $[R_{ch}/(R_{ch}+d)]^3$, where d is the radial distance from the chamber wall (e.g., Dragoni and Magnanensi 1989). The total differential stress ($\triangle P_{ch} - \sigma_h$) on the wall rocks at the chamber margin is $1.5\triangle P_{ch}$ (cf. McLeod and Tait 1999).

Rearranging Eq. (4), we obtain the following differential equation describing the time–evolution of $\triangle P_{ch}$:

$$\frac{1}{E}\frac{d\Delta P_{ch}}{dt} = \frac{2}{R_{ch}}\frac{dR_{ch}}{dt} - \frac{\Delta P_{ch}}{\mu_{wr}}. \quad (6)$$

An influx of buoyant magma from a deeper source through a dike causes the chamber to expand. The pressure driving the new magma into the chamber is (presumably) limited by the height of the underlying magma column, and is unlikely to exceed about 400 MPa (see Fig. 2). Assuming the magma is incompressible, the rate of change of chamber radius can be expressed in terms of the magma influx $Q(t)$ and chamber radius R_{ch} or volume V_{ch}

$$\frac{2}{R_{ch}}\frac{dR_{ch}}{dt} = \frac{Q(t)}{2\pi R_{ch}(t)^3} = \frac{2Q(t)}{3V_{ch}(t)}. \quad (7)$$

Substituting Eq. (7) into Eq. (6) leads to the governing equation for the rate of change of magma chamber overpressure:

$$\frac{1}{E}\frac{d\Delta P_{ch}}{dt} = \frac{2Q(t)}{3V_{ch}(t)} - \frac{\Delta P_{ch}}{\mu_{wr}} \quad (8)$$

Thus, the buildup of excess pressure in the chamber depends on the relative contributions of the elastic and viscous strain rates. If $\triangle P_{ch}$ is initially zero, the elastic strain rate will dominate at the start of a replenishment episode and $\triangle P_{ch}$ increases in proportion to Q/V_{ch}. The chamber overpressure will increase until it is relieved through the fracturing of bounding wall rocks or dike formation, which may, in turn, lead to eruption. However, over time, and depending on μ_{wr}, the viscous strain rate eventually increases to match the total strain rate. In this regime, chamber overpressure drives steady-state radial creep in the wall rocks, and $\triangle P_{ch}$ approaches a constant.

The maximum overpressure, corresponding to the condition $d\triangle P_{ch}/dt=0$ is

$$\Delta P_{\max} = \frac{2\mu_{wr}Q}{3V_{ch}} \quad (9)$$

where Q is the time-averaged magma influx and V_{ch} is the chamber volume. Consequently, if μ_{wr} can be estimated, the maximum magma chamber overpressure as a function of Q/V_{ch} can be readily obtained. In the following analysis, we evaluate $\triangle P_{\max}$ for a range of plausible wall-rock viscosities and also power law behavior (e.g., Brace and Kohlstedt 1980; Kirby 1980, 1983, 1985; Carter and Tsenn 1987).

Magma chamber pressurization time scales: "elastic" versus "viscous" regimes

Equation (8) can also be written in the form:

$$\frac{d\Delta P_{ch}}{dt} = \frac{E}{\mu_{wr}}(\Delta P_{\max} - \Delta P_{ch}) \quad (10)$$

and applied in two asymptotic limits to define two time characteristic scales for chamber pressurization. When $\triangle P_{\max}$ is much greater than the overpressure needed to propagate a dike, $\triangle P_{\text{crit}}$, the wall rocks are effectively elastic and viscous deformation is unimportant. In this "elastic regime", the time required to pressurize the chamber to the critical pressure can be determined from:

$$\tau_e = \frac{\Delta P_{crit}}{(d\Delta P_{ch}/dt)_e} = \frac{3\Delta P_{crit}V_{ch}}{2QE} \quad (11)$$

As will be discussed, this limit clearly applies in many circumstances and, given the constraints on Q discussed above, the implied dependence of τ_e on chamber volume may be important for interpreting the frequency of eruptions in volcanic systems.

In the alternative limit we define as the "viscous regime", $\triangle P_{\max} \leq \triangle P_{\text{crit}}$, and radial creep in the wall rocks (Carter and Tsenn 1987) is important. Thus, the time scale to pressurize the magma chamber is

$$\tau_v = \frac{\mu_{wr}}{E} \quad (12)$$

which is the viscoelastic relaxation time (i.e., the "Maxwell time"). Explicitly, τ_v is dependent only on the wall-rock properties. However, if μ_{wr} depends on strain rate and temperature (discussed below), τ_v is also dependent on chamber volume.

Pressurization of a pre-existing magma-filled crack

In the model of McLeod and Tait (1999), dikes form due to magma being forced into pre-existing magma-filled cracks in the wall of a chamber. The pressurization of the magma in the crack lags behind the pressurization of the magma in the chamber because of the time required for magma to flow from the chamber into a dilating crack. Magma flow from the chamber into a crack is driven by the difference between the pressure in the chamber, Pch,

and the pressure in the crack, P_d, and is retarded by viscous stresses governed by the viscosity of the magma μ_m and the width of the crack. The initial P_d can be equal to the ambient lithostatic pressure σ_r, the hoop stress σ_h, or a value in between. McLeod and Tait (1999) derive the following equation that describes the evolution of dike pressure with time (using our notation):

$$\frac{dP_d}{dt} = \frac{(P_d - \sigma_h)^3}{3E^2\mu_m}(P_{ch} - P_d). \tag{13}$$

Using our definition of the chamber over pressure, $\Delta P_{ch} = (P_{ch} - \sigma_r)$, and defining the "dike overpressure", $\Delta P_d = (P_d - \sigma_h)$, Eq. (13) can be rewritten in terms of the chamber overpressure and the dike overpressure:

$$\frac{d\Delta P_d}{dt} = \frac{\Delta P_d^3}{3E^2\mu_m}\left(\frac{3}{2}\Delta P_{ch} - \Delta P_d\right) \tag{14}$$

Equations (10) and (14) are the governing equations for the time evolution of the chamber and dike overpressures when the wall rocks have a Maxwell viscoelastic rheology. The equations apply only up to the point that the dike begins to propagate. Once propagation commences, additional equations are needed to describe the flow of magma into the propagating dike (e.g., Lister and Kerr 1991) and to account for the effect of magma loss from the chamber on the chamber overpressure. Our model should, however, be adequate to determine whether a particular set of initial conditions (Q and V_{ch}) and material properties (E, μ_{wr}, μ_m) will produce chamber overpressure sufficient to propagate a nascent rhyolitic dike to the surface (10–40 MPa), and to determine the timescales for changes in chamber and dike overpressure.

Although Eqs. (10) and (14) completely describe the problem as posed, additional insight can be gained by further non-dimensionalizing the equations. We define $\mathbf{p}_d = \Delta P_d/\Delta P_{\max}$ and $\mathbf{p}_{ch} = \Delta P_{ch}/\Delta P_{\max}$ and rewrite Eqs. (10) and (14) to obtain:

$$\frac{d\mathbf{p}_{ch}}{dt} = \frac{E}{\mu_{wr}}(1 - \mathbf{p}_{ch}) \tag{15a}$$

$$\frac{d\mathbf{p}_d}{dt} = \frac{\Delta P_{\max}^3}{3E^2\mu_m}\mathbf{p}_d^3\left(\frac{3}{2}\mathbf{p}_{ch} - \mathbf{p}_d\right). \tag{15b}$$

Equations (15a) and (15b) identify the two time scales that govern the dynamics of dike formation: the Maxwell time, τ_v [cf. Eq. (12)] and the time scale for pressurization of a dike,

$$\tau_d \sim \frac{3E^2\mu_m}{\Delta P_{\max}^3}, \tag{16}$$

which is evident in the closed-form solution of McLeod and Tait (1999) for the case of a constant hoop stress and chamber over-pressure. The solution to Eq. (15b) collapses the results of McLeod and Tait to a single curve (Fig. 3a). Note that the initial value of $\triangle P_d$ for this model is $1/2\triangle P_{ch}$ and the final value is $3/2\triangle P_{ch}$, which follows if it is assumed that the initial dike pressure is equal to σ_r

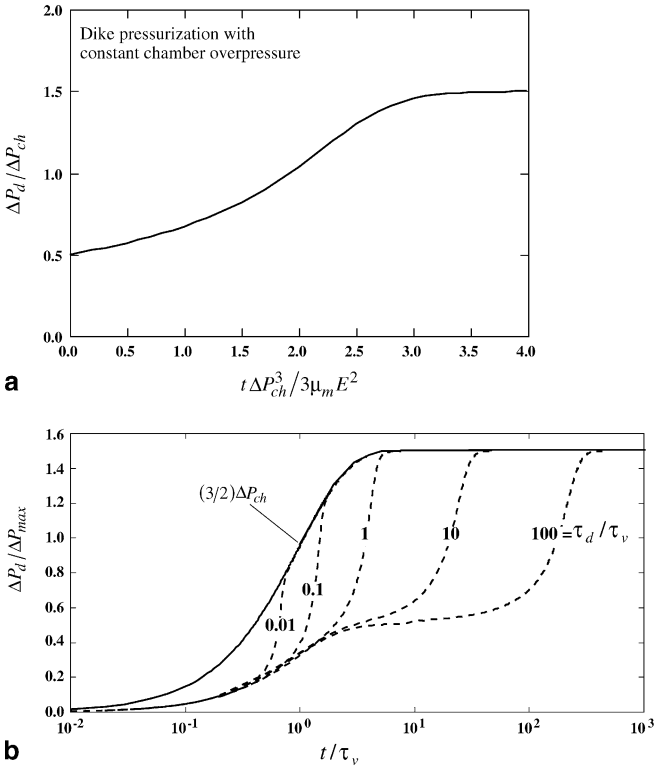

Fig. 3 **a** Dimensionless version of the McLeod and Tait (1999) model of dike pressurization following an instantaneous increase in magma chamber pressure. The lag in the time to pressurize a preexisting magma-filled crack (i.e., the "dike pressurization time scale", τ_d) is governed strongly by the chamber pressure and the magma viscosity, which determine the flow rate from the magma chamber into the crack. **b** Non-dimensional representation of the relationship between dike pressurization and magma chamber pressurization for the model of a constant magma influx to the chamber and Maxwell viscoelastic wall-rock rheology. The time lag between chamber and dike pressurization is governed by the ratio of the dike pressurization time, τ_d, to the time scale for chamber pressurization in the viscous regime, τ_v, which is also the Maxwell viscoelastic relaxation time

cf. Eq. (5). Figure 3a shows that the dike overpressure responds slowly over a time $t \leq \tau_d$, after which point the overpressure will increase rapidly towards $1.5\triangle P_{ch}$.

Non-dimensionalizing time in Eq. (15a) according to $t'=t/\tau_v$ leads to a simplified form of the governing equations:

$$\frac{d\mathbf{p}_{ch}}{dt'} = (1 - \mathbf{p}_{ch}) \tag{17}$$

$$\frac{d\mathbf{p}_d}{dt'} = \frac{\tau_v}{\tau_d}\mathbf{p}_d^3\left(\frac{3}{2}\mathbf{p}_{ch} - \mathbf{p}_d\right) \tag{18}$$

which show the dependence of the evolution of dike overpressure on the ratio τ_v/τ_d. The solutions to Eqs. (17) and (18) are plotted in Fig. 3b. When $\tau_d < \tau_v$ dike pressure increases rapidly to match the chamber overpressure even at low values of the chamber overpressure. Consequently, the dike pressure approaches the maximum pressure on the time scale for chamber pressurization τ_v . When $\tau_d > \tau_v$

dike pressurization is delayed in comparison to chamber pressurization, and the time scale for the dike pressure to approach the maximum is approximately τ_d.

The solutions to Eqs. (17) and (18) were obtained numerically assuming a constant $\triangle P_{\max}$. However, the increase in the chamber volume with time caused by a constant influx of new magma Q causes a slow reduction in the maximum chamber overpressure $\triangle P_{\max}$ during the pressurization of the chamber and dike. For our purposes this approximation is appropriate because the time scale for the change of $\triangle P_{\max}$ for magma chambers that are moderately large ($R \geq 4$ km) is much longer (order 10^5 years) than either τ_d or τ_v as estimated below.

Application of the model

Constant magma supply with uniform wall-rock viscosity

Figure 4 shows the maximum chamber overpressure $\Delta P_{\max}$ plotted against chamber volume V for Q= 0.005 km^3 year^{-1} and for wall-rock viscosities of 10^{17}–10^{20} Pa s^{-1}. The value of Q used for this calculation is higher than the nominal rate of accumulation of high silica magma in many systems (0.002 km^3 year^{-1}) and, hence, can account for a significant amount of crystallization of more mafic magma that might be feeding the chamber. For small magma chambers (less than 10–10^2 km^3) and higher viscosity wall rocks (μ_{wr} >10^{20} Pa s^{-1}) the stresses required to cause fracturing of the wall rocks (ca. 50 MPa) or the propagation of rhyolite dikes to the surface (10–40 MPa) are attained readily. Thus, the replenishment of small magma chambers, unless they are contained in country rocks with a low effective viscosity, will probably lead to eruption. The periodicity and volume of the eruptions will likely be determined by the rate of replenishment and the volume of magma that must be drained from the chamber to relieve overpressure (e.g., Tait et al. 1989; Bower and Woods 1997). In contrast, for large magma chambers (>10^2 km^3) and wall-rock viscosities of about 10^{19} Pa s^{-1} or less, radial creep in the wall rocks inhibits the chamber from becoming sufficiently pressurized to generate rhyolite dikes that propagate to the surface. Consequently, the magma supplied to the chamber will tend to accumulate, causing the chamber to grow progressively in volume.

These results imply that once chambers become sufficiently large, silicic volcanism should cease, despite a continuous supply of new magma from deeper levels. However, eruptions may be possible in this storage regime if much larger values of Q can be generated temporarily, or if stresses can be concentrated locally along the chamber walls (see discussion below).

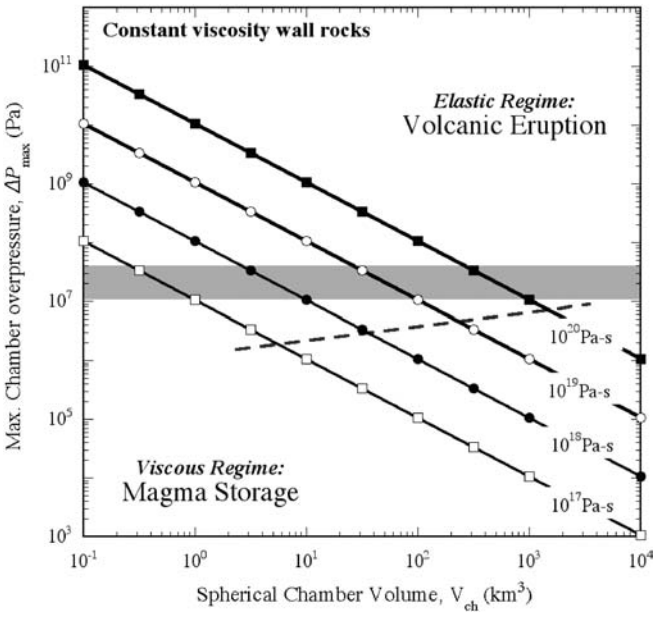

Fig. 4 The maximum chamber over-pressure, $\Delta P_{\max}$, generated by a constant magma influx, Q=0.005 km^3 year^{-1}, as a function of chamber volume, V_{ch}, for a spherical chamber with wall rocks with a constant viscosity. The *shaded region* shows the probable range of critical dike overpressures, $\Delta P_{crit} = 10 - 40$ MPa, required to propagate a rhyolite dike to the surface. Curves are shown for various wall-rock viscosities. If $\Delta P_{\max} > \Delta P_{crit}$, the chamber is approximately in the elastic regime and dike formation is expected to lead to volcanic eruption. Conversely, if $\Delta P_{\max} < \Delta P_{crit}$, the chamber is approximately in the viscous regime, which favors magma storage and the growth of large magma chambers. The dashed line indicates the influence of magma buoyancy on $\Delta P_{\max}$ (see text for discussion)

Constant magma supply with power law wall-rock rheology

The results of rock mechanics experiments show that at elevated temperatures and confining pressures, crustal rocks flow by solid-state creep. The rheology of the wall rocks is described by the Weertman relation (e.g., Brace and Kohlstedt 1980; Kirby 1980, 1983, 1985; Carter and Tsenn 1987):

$$\left(\frac{d\varepsilon}{dt}\right)_v = Ae^{-G/MT}\sigma_v^n \tag{19}$$

Here, A is a constant that depends on the material, T is absolute temperature, G is the activation energy for creep, n is the power law exponent, σ_v is the deviatoric stress, and M is the molar gas constant. The deviatoric stress is mechanically equivalent to the flow stress in the wall rocks, σ_{wr} (cf. the section Thermal survival of dikes and wall-rock rheology). The most compelling feature of this approach to wall-rock rheology is that the effective wall-rock viscosity is an explicit function of temperature and strain rate. In order to keep our analysis simple we only use representative values of the strain rate and temperature to estimate the flow stress of the wall rocks. For purposes of illustration, we use the strain rate in the wall

rocks at a distance $R_{ch}/2$ from the chamber wall, and evaluate the flow stress as a function of temperature. This gives the following expression for the maximum chamber overpressure:

$$\Delta P^{PL}_{\max} \approx \frac{2}{3}\left(\frac{16Q(t)}{81AV_{ch}(t)}e^{G/MT}\right)^{1/n} \quad (20)$$

where the superscript "*pl*" means "power law" and we have substituted the flow stress of the wall rocks for the deviatoric stress according to

$$\sigma_{wr}(R_{ch}) = \frac{3}{2}\Delta P_{ch} \quad (21)$$

We use the material properties determined for Westerly granite with 0.1 wt% water (Hansen and Carter 1983) to represent the wall rocks: A=2×10^{-4} MPa$^{-1.9}$ s^{-1}, G=141 kJ mol^{-1}, and n=1.9. The experiments that were used to define the parameters were carried out at temperatures of 546 to 740 °C, a confining pressure of 1 GPa, and strain rates in the range 10^{-5} to 10^{-7} s^{-1}. Plausible conditions for a magma chamber emplaced in the crust at depths between 15 and 5 km are T=200–600 °C, σ_r=0.15–0.4 GPa, and strain rates between about 10^{-9} and 10^{-14} s^{-1}. The effective viscosity, $\mu^{pl}_{wr} = \sigma_{wr}/3(d\varepsilon/dt)$, is 10^{17}–10^{22} Pa s^{-1}.

$\Delta P^{pl}_{\max}$ and μ^{pl}_{wr} are plotted as a function of V_{ch} in Fig. 5a, b, and μ^{pl}_{wr} is plotted against the radial strain rate $(d\varepsilon/dt)$ in Fig. 5c. Whereas varying Q has a small effect since $\Delta P^{pl}_{\max}$ and μ_{wr} depend approximately on $Q^{1/2}$, $\Delta P^{pl}_{\max}$ and μ^{pl}_{wr} depend strongly on the strain rate and temperature. In particular, $(d\varepsilon/dt)$ decreases by five orders of magnitude, from a little less than 10^{-9} s^{-1} to less than 10^{-14} s^{-1}, as the chamber volume grows from 0.1 to 10^4 km^3. At constant strain rate, $\Delta P^{pl}_{\max}$ decreases by around a factor of 200 between 300 and 600 °C.

Finally, the results shown in Figs. 4 and 5a are similar. For small magma chambers (less than 10–100 km^3) and relatively cool wall rocks (<400 °C), $\sigma_{wr} \gg \Delta P_{crit}$ and dike formation is expected to cause volcanic eruptions. In contrast, for large magma chambers (>100 km^3) and wall-rock temperatures in excess of 300 to 350 °C, $\sigma_{wr} < \Delta P_{crit}$ and dikes are not expected to propagate to the surface.

Comments on wall-rock viscosity

An important question is whether it is reasonable to expect wall-rock temperatures such that $\sigma_{wr} \leq \Delta P_{crit}$. For a geothermal gradient of 20 °C km^{-1}, say, which may be typical of cratonic crust, the ambient temperature at depths of 5 to 15 km are in the range 100 to 300 °C and $\sigma_{wr} > \Delta P_{crit}$. However, if a sufficient amount of magma traverses the crust or is emplaced as dikes and sills, the wall-rock temperatures are likely to increase over time such that $\sigma_{wr} < \Delta P_{crit}$, resulting in conditions more favorable for magma storage.

In general, batholiths and silicic volcanic systems that produce large silicic magma chambers are in regions in which the heat flow substantially exceeds that typical of cratonic continental crust. Hence, it is not unreasonable to expect that effectively viscous deformation of wall rocks will influence the dynamics governing the formation of dikes from large magma bodies (or small magma bodies emplaced into warm or weak rocks). Furthermore, it may not be necessary for the entire wall rock envelope to be in the viscous regime. If $\sigma_{wr} < \Delta P_{crit}$ for a substantial fraction of the chamber walls (e.g., the lower half of a pluton) resultant viscous flow may prevent any part of the chamber from reaching a critical overpressure.

The effective viscosity of crustal rocks above a magma chamber has been estimated using geodetic measurements of surface deformations on the resurgent dome in the Long Valley caldera (Newman et al. 2001). The best fit to the data is achieved with a Maxwell viscoelastic model and an effective wall-rock viscosity in the range 10^{15}–10^{18} Pa s^{-1}. In their preferred model, the authors choose an intermediate value of 10^{16} Pa s^{-1}, which is much lower than we calculate (Figs. 4 and 5), and also much lower than the typical values of 10^{19}–10^{21} Pa s^{-1}, which are usually taken to be applicable to the upper 10 km of continental crust (Carter and Tsenn 1987; Bills et al. 1994). The Newman et al. (2001) results suggest that magma chamber wall rocks can have relatively low effective viscosities and, thus, that viscous deformation is likely to be important. Recent studies have also shown that pervasive fractures or "damage" to the host rock during dike propagation or faulting (Lyakhovsky et al. 1993; Agnon and Lyakhovsky 1995; Lyakhovsky et al. 1998, 1997; Meriaux et al. 1999) further reduce the effective viscosity of the wall rocks. In addition, metamorphic reactions in the potentially fluid-rich environment around a high level pluton may also contribute to weakening the wall rocks (Rubie 1983). Therefore, our conclusion is that the properties of wet Westerly granite are reasonable, if not conservative, for evaluating our model. It is clear that the wall rocks could be significantly weaker in many instances.

Time scales for dike formation

Our analysis indicates that the time scales for chamber pressurization (τ_v or τ_e) determine the time needed to form a dike. For constant Q, the time scale for dike pressurization, τ_d (cf. McLeod and Tait 1999), is unlikely to play a role because it is significant only for unrealistically high values of the magma viscosity. This conclusion is reached by considering the conditions necessary for τ_d to be larger than τ_v or τ_e. In the viscous regime, the condition $\tau_d > \tau_v$ leads to the following:

$$\mu^{crit}_m > \frac{\mu_{wr}}{3}\left(\frac{\Delta P_{\max}}{E}\right)^3 > \frac{\mu_{wr}}{3}\left(\frac{\Delta P_{crit}}{E}\right)^3, \quad (22)$$

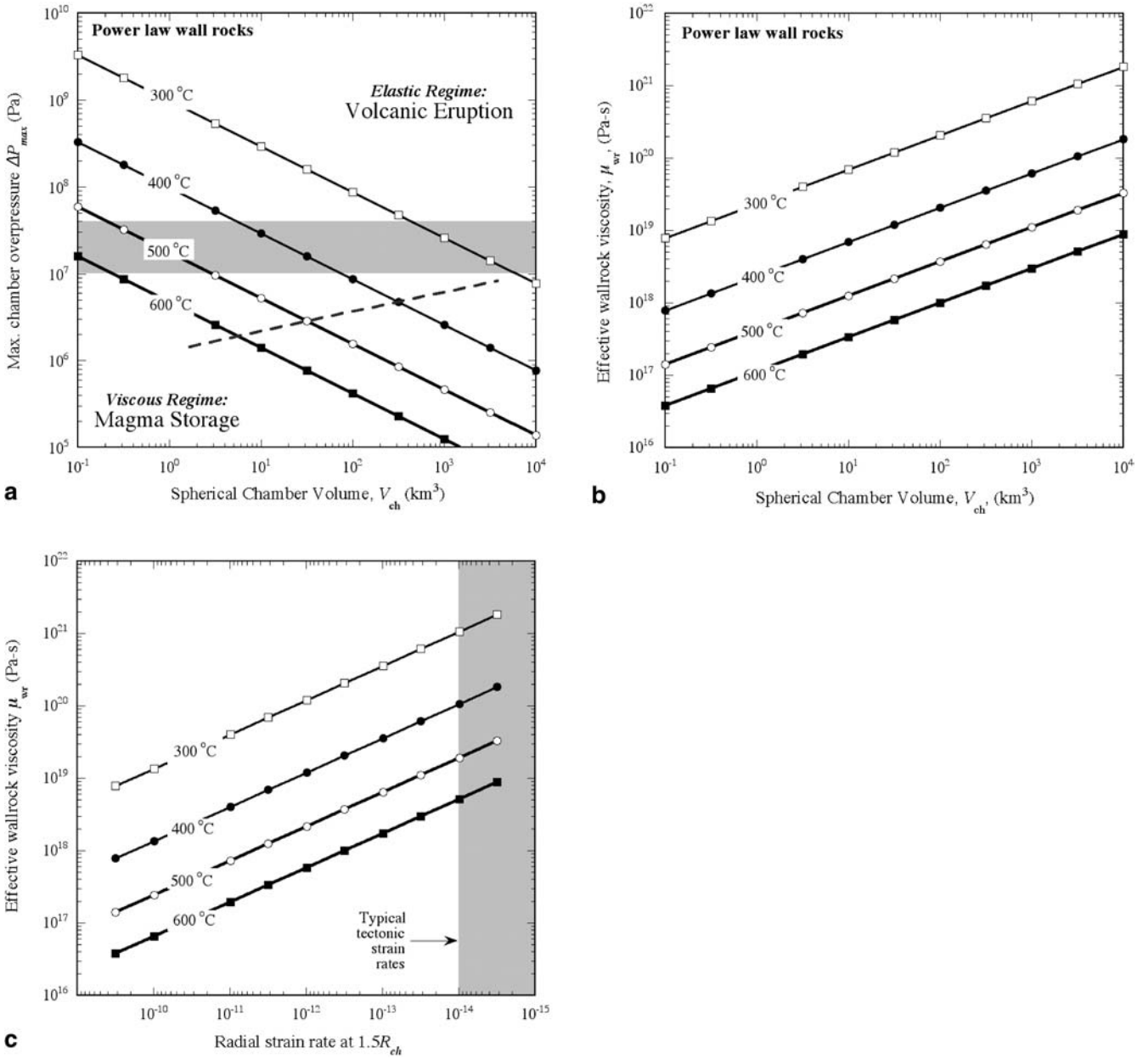

Fig. 5 **a** The maximum chamber over-pressure, $\Delta P_{\max}$, generated by a constant magma influx, Q=0.005 km^3 year^{-1}, as a function of chamber volume, V_{ch}, for a spherical chamber contained in wall rocks with a power law rheology. The wall rocks are taken to be Westerly granite with 0.1% water (e.g., Hansen and Carter 1983). In a way similar to Fig. 4, the *shaded region* shows the probable range of critical dike overpressures, $\Delta P_{crit} = 10 - 40$ MPa, required to propagate a rhyolite dike to the surface and delineates regimes leading to magma storage or volcanic eruption. Whether an influx Q leads to volcanism or storage depends on both the volume of the chamber and temperature of the wall rocks. **b**, **c** Plots of the effective wall-rock viscosity, μ_{wr}, as a function of chamber volume, V_{ch}, and radial strain rate $(d\varepsilon/dt)$. The *dashed lines* in **a** indicate the influence of magma buoyancy on $\triangle P_{\max}$ (see text for discussion)

where the second inequality recognizes that if $\triangle P_{\max}$ is not greater than $\triangle P_{\text{crit}}$, no dike can form. Substituting appropriate values (μ_{wr}=10^{19} Pa s^{-1}, $\triangle P_{\text{crit}}$=$2\times10^7$ Pa and E=10^{10} Pa) yields the condition $\mu_m^{crit} > 2 \times 10^{10}$ Pa s^{-1}, which is about two to four orders of magnitude greater than the likely upper limit for typical (water-saturated) rhyolitic magmas (Bottinga and Weill 1972; Shaw 1972; Anderson et al. 1989; Wallace et al. 1995; Hess and Dingwell 1996). Similarly, in the elastic regime the condition $\tau_d > \tau_e$ leads to:

$$\mu_m^{crit} > \frac{3\Delta P_{crit} V_{ch}}{2Q}\left(\frac{\Delta P_{crit}}{E}\right)^3. \qquad (23)$$

For Q=0.005 km^3 year^{-1}, $\mu_m^{crit} = 1.5 \times 10^8$ Pa s^{-1} only for small magma chambers (V_{ch}=0.1 km^3). Hence, in the elastic regime, τ_d is important only for very high values of

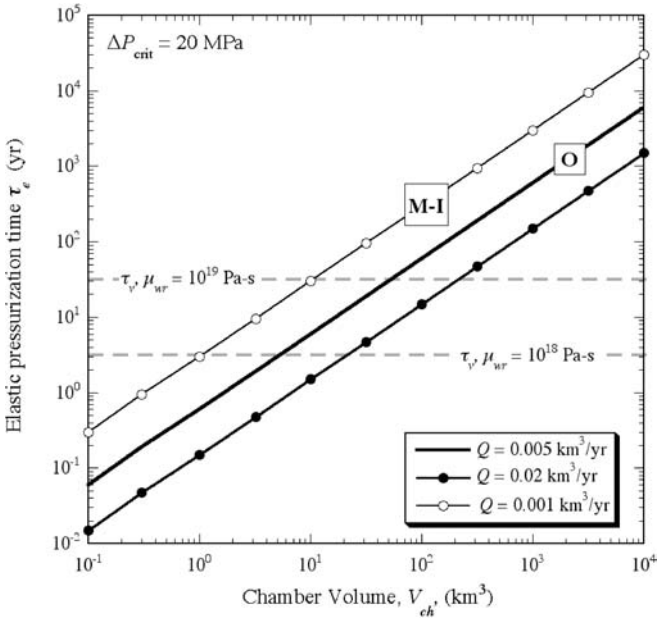

Fig. 6 The time scale for chamber pressurization in the elastic regime, τ_e, versus chamber volume for different values of the magma influx to the chamber. The viscous time scale for chamber pressurization, τ_v, which depends only on material properties of the wall rocks, is shown for reference for two wall-rock viscosities. If magma chambers are initially at lithostatic pressure and are in a regime in which dikes can form τ_e gives, approximately, the amount of time to pressurize a chamber to the critical overpressure, ΔP_{crit}, required to propagate a rhyolite dike to the surface. Hence, τ_e indicates also the minimum repose time between successive eruptions. Also shown are conditions inferred for the Okataina volcanic complex (*O*), New Zealand and the Mono–Inyo (*M–I*) volcanic chain in the Long Valley caldera, CA. Assuming that the observed frequency of (small volume, non-CCF) eruptions indicates τ_e, we apply measurements of eruption volumes to constrain, in turn, the long-term magma supply, *Q*, and the volume of the chamber prior to an eruption (see text for discussion)

Q/V_{ch} and only for very viscous magmas. Overall, it appears that τ_d is unimportant for most likely conditions in our model.

Dike frequency and episodic magma supply

The elastic chamber pressurization time, τ_e, is plotted against chamber volume, *V,* in Fig. 6. For small, initially unpressurized, chambers τ_e can be interpreted to be the amount of time required to pressurize a chamber to the critical overpressure $\triangle P_{crit}$. Assuming that eruption relieves the chamber overpressure τ_e is then the minimum time period between successive dikes, and hence should approximate the minimum time between eruptions.

Direct observations of volcanic eruptions (e.g., Richter et al. 1996), as well as measurements of ground displacements before, during, and after eruptions (e.g., Dvorak and Dzurisin 1997), indicate that injections of new magma can be episodic and have flow rates that vary strongly in time (e.g., Wadge 1980). In addition, it has been suggested that sudden increases in chamber storage rate may lead to volcanic eruptions on Hawaii (Cayol et al. 2000). Hence, it is useful to consider the influence of episodic injections on dike formation—particularly in large magma chambers in which reasonable long-term values for *Q* do not lead to dike propagation to the surface.

For large magma chambers in the viscous regime, dikes can form only if the magma influx substantially exceeds the long-term average value *Q*. The minimum influx, Q_{min}, necessary to generate a dike in a chamber of volume, V_{ch}, is given by:

$$Q_{\min} = \frac{3V_{ch}}{2\mu_{wr}}\Delta P_{crit}. \tag{24}$$

In order for ΔP_{max} to approach ΔP_{crit} this flux must be maintained for a time roughly equal to the time scale, τ_v, for chamber pressurization in the viscous regime (cf. Fig. 3b) and, thus,

$$\Delta V_{\min} \approx Q_{\min}\tau_v \tag{25}$$

At the typical long-term supply rate *Q*, the time to produce this magma and store it at deeper levels before injection into the chamber is:

$$\Delta t_{\min} \approx \frac{\Delta V_{\min}}{Q} = \tau_e. \tag{26}$$

Thus, for large magma chambers in the viscous regime, as well as for small chambers in the elastic regime, the elastic pressurization time scale gives an estimate for the minimum time between eruptions, which should be simply proportional to *Vch*/*Q*, assuming that $\triangle P_{crit}$ and *E* are constant.

Other mechanical considerations

Magma buoyancy

In the foregoing analysis, the influence of the buoyancy of silicic magma on the overpressure in the magma chamber is neglected. The additional overpressure due to magma buoyancy depends on the height of the buoyant magma layer and the density structure in the surrounding crust. In the simple case of a spherical magma chamber composed only of incompressible silicic magma the chamber overpressure will increase vertically along the chamber walls and have a maximum of $\triangle \rho g R$ at the top of the body. Thus, for a density difference, $\Delta\rho$=250 kg m^{-3} (Petford et al. 1994), ΔP_{max} can be increased by 2.5 to 25 MPa, say, for *R*=1 to 10 km. The influence of buoyancy on ΔP_{max} is indicated in Figs. 4 and 5a, and it is apparent that buoyancy may be important for producing dikes from very large magma chambers that are otherwise in the viscous regime. However, if larger chambers tend to become flattened or are layered with silicic magma underlain by neutrally-buoyant more mafic magma, as suggested by the data shown in Fig. 7 (see discussion below), the maximum thickness of a buoyant magma

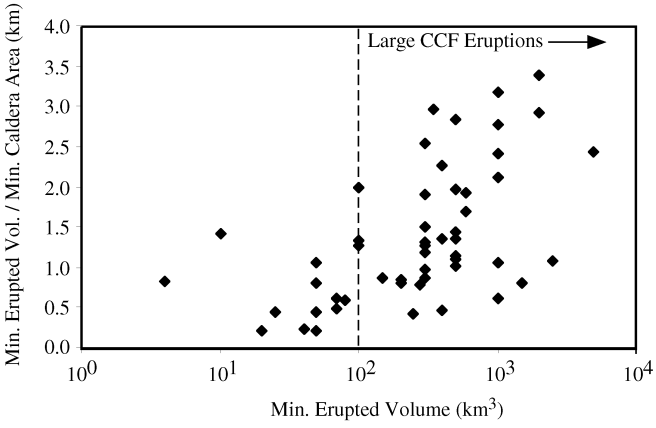

Fig. 7 Plot of minimum erupted volume caldera area vs. minimum erupted volume for rhyolitic eruptions around the world. The largest cataclysmic caldera-forming (CCF) eruptions typically have volumes that significantly exceed 100 km^3 and were erupted from magma chambers in which silicic magma layers were around 0.5 – 3 km thick.

layer may be 0.5–3 km, corresponding to an additional overpressure of 1–10 MPa. Thus, magma buoyancy is likely important for the dynamics of dike formation in the largest magma chambers (Figs. 4 and 5a) and may even provide an upper limit to the vertical size of silicic magma chambers.

Regional extension

Tectonic extension could influence dike formation in two ways. Extension can suppress dike formation by increasing the volume of the chamber and dissipating chamber overpressure. On the other hand, extension can enhance dike formation by stretching the roof and floor rocks at a rate sufficient to cause tensile failure.

Whether or not the roof rocks fail in tension during tectonic extension depends on the magnitude of the resultant flow stresses in comparison to the failure strength of the rock. This can be evaluated from Fig. 5c. Typical tectonic strain rates are in the range 10^{-14}–10^{-15} s^{-1} (Carter and Tsenn 1987). Under these conditions, rocks under substantial confining pressure and at temperatures above 300 °C should flow rather than fracture. Hence, tectonic extensional strains will likely not fracture the hot rocks near the pluton.

In the viscous regime, extension should enhance the chamber overpressure at the sides of the chamber aligned with the direction of the least principle compressive regional stress by an amount equal to the deviatoric tensile stress in that direction. Extension will concomitantly decrease the chamber overpressure in the plane perpendicular to the direction of extension. Hence, with an influx of new magma it will be possible to expand the chamber in the direction of extension without generating overpressure anywhere but along the two sides of the pluton aligned with the extension direction. For a chamber with an elliptical cross section the influx, Q_{ex}, necessary to balance the negative chamber overpressure in the plane perpendicular to the extension direction is the rate of change of chamber volume due to expansion along the long axis. This condition can be shown to be: $Q_{ex} = \dot{\varepsilon}_{ex} V_{ch}$, where the subscript "*ex*" denotes extension and $\dot{\varepsilon}_{ex}$ is the tectonic strain rate. For a plausible strain rate of 10^{-14} s^{-1} Q_{ex} is negligible for small chambers, but approaches the expected values of Q as the chamber volume approaches 10^4 km^3. As a result, extension has little effect on the chamber overpressure generated by a magma influx into small chambers. In contrast, for large chambers, extension can significantly decrease the overpressure at the top of the chamber, leading to an enhanced suppression of dike formation.

The stresses maintained in hot crustal rocks at the strain rates characteristic of regional tectonism are of order 10 MPa (Fig. 5c), and are comparable to ΔP_{crit}. In general, however, extension should make dike generation from the tops of plutons even less likely when viscous deformation is significant. Extension is also expected to increase the likelihood of dike formation at the sides of chambers that are aligned with the extension direction, which may augment the lateral growth of magma chambers.

Crystallization in the magma chamber

The influence of solidification on the volume of stored magma cannot be neglected for the large magma bodies that supply CCF eruptions; crystallization is in fact needed in order to produce the high silica compositions of many of the erupted magmas. We present a simplified analysis to show that crystallization rates compete with magma supply for large chambers. The extent to which crystallization reduces the magma accumulation rate depends on a balance between the heat carried into the chamber by the new magma, the heat loss to the wall rocks, and the rate at which latent heat is produced by crystallization.

Assuming the magma to be on its liquidus with some crystals, the ratio of the crystallization rate, Q_{xl}, to the magma influx, Q, can be expressed as:

$$\frac{Q_{xl}}{Q} \approx \frac{qS}{Q\rho L} - \frac{c\Delta T}{L}, \tag{27}$$

where ρ and c are the density and specific heat of the magma, q is the average heat flux at the walls of the chamber, S is the surface area of the chamber, and $\triangle T$ is the temperature difference between the new and resident magmas. The approximate sign is used because Eq. (27) does not account for enthalpy of mixing or for compositional effects on the liquidus temperature (cf. DePaolo et al. 1992; Jellinek and Kerr 1999). The critical surface area at which crystallization will be sufficiently fast to maintain a steady-state volume fraction f of crystals in the chamber (this is met if Q_{xl}=fQ) is:

$$S_{crit} = \frac{Q\rho(fL + c\Delta T)}{q}. \quad (28)$$

Consequently, solidification rates are sufficient to increase the volume fraction of crystals in a chamber only when the chamber surface area $S \geq S_{crit}$. In the simple case of a spherical magma chamber with radius R, Eq. (28) becomes:

$$R_{crit} = \left[\frac{Q\rho}{4\pi q}(fL + c\Delta T)\right]^{1/2}. \quad (29)$$

Thus, for a given magma chamber size, a lower influx of new magma is needed to maintain a magma with a high crystal content than to maintain one with a low crystal content.

Studies of the heat flux from active magmatic systems in Iceland (Palmaesson and Saemundson 1974), Yellowstone caldera (Fournier and Pitt 1985), and the Taupo Volcanic zone, New Zealand (Bibby et. al. 1995), indicate similar cooling rates and a surface heat flux q in the range 0.2 to 0.8 W m^{-2}. For a magma influx Q=0.005 km^3 year^{-1}, $\triangle T$=100–300 °C, q=0.5 W m^{-2}, a critical chamber radius of 3 to 6 km is obtained for f=0.1 to 0.5. The corresponding critical chamber volume is between 100 and 900 km^3.

Hence, crystallization does not greatly affect the magma accumulation rate until magma bodies reach a volume corresponding to a large CCF eruption. Once the chamber volume becomes large, the maintenance of eruptible magma requires a large value of Q. In order to maintain a chamber with a volume greater than 1,000 km^3, it is necessary that Q/q be significantly higher than the values we have used here, and it is also likely that eventually the rate of crystallization becomes higher than the magma influx.

Geometric effects in non-spherical chambers

Figure 7 shows data from a large number of caldera systems (Lipman 1984) and indicates that the thickness of the layer of magma erupted in large CCF eruptions is only about 0.5 to 3 km, roughly a factor of ten smaller than the maximum horizontal dimension of the caldera. These data suggest that large magma chambers are flattened in the vertical direction, and (or) that the thickness of low-density magma in the chamber is small compared to the total chamber height. In the case of a magma chamber shape that departs radically from spherical, the stresses generated by inflation of the chamber are non-uniform. One way to generate dikes from a large chamber is if there are regions of stress concentration along the chamber walls. For a flattened, disc-shaped chamber, replenishment might result mainly in lateral spreading of the chamber. Hoop-stresses and strains might then be concentrated locally at the lateral edges of the chamber, which would behave effectively like chambers of smaller radius, allowing dikes to form around the periphery of the chamber. Thus, we would expect large disc-shaped chambers to leak silicic magma to the surface mainly at the margins. This idea is consistent with the observations at Long Valley, for example, where the pre-caldera lavas and tuffs of Glass Mountain were erupted from vents that define an arcuate trend along the eastern edge of the caldera. At Jemez, New Mexico, post-caldera dacites were erupted in a ring corresponding closely to the outline of the caldera (Smith and Bailey 1968; Bailey et al. 1976).

Discussion

Evolution of wall-rock rheology: role of "preheating"

Our model allows us to relate the eruptive behavior of silicic volcanic systems to wall-rock rheology, magma supply, and magma chamber volume. Indeed, the rheology of the wall rocks may be particularly important. For the range of strain rates we have identified to be appropriate, shallow crustal rocks will presumably behave in an effectively viscous way only if a substantial volume of rock enclosing the magma chamber is heated to well above the normal geotherm.

Thus, the constant or episodic replenishment of newly-formed magma chambers in relatively cold wall rocks is expected to lead to dike formation and volcanic eruptions. With prolonged magmatic activity and/or after an extended time after emplacement of a magma body, however, the wall rocks may become sufficiently warm that viscous effects become important. Consequently, one prediction of the model is that large, shallow silicic magma chambers are likely to form only after a protracted period of precursory volcanism during which wall rocks are "pre-heated." A maximum time for preheating is the time scale for thermal diffusion across a 1–2-km thickness of rock, say, which is about 50,000 to 200,000 years. This time scale may be reduced if, for example, convective heat transfer in a spatially extensive hydrothermal system is important or if a large number of dikes traverse the wall rocks within a distance comparable to the radius of the chamber.

It is generally observed that large caldera-forming (CCF) eruptions occur in volcanic systems that have been active for an extended period of time. For example, at Long Valley, California, the Bishop Tuff formed more than 10^6 years after the initiation of the rhyolitic volcanism of Glass Mountain. In the Okataina volcanic center, Taupo volcanic zone, New Zealand, large CCF eruptions of the Matahina and Rotoiti ignimbrites at 280 and 60 ka, respectively, were each preceded by (1–10 km^3) dome-forming and pyroclastic eruptions, the most notable of which have produced the Tarawera and Haroharo volcanic complexes (Bailey 1965; Davis 1985; Bailey and Carr 1994; Schmitz 1995; Wilson et al. 1995; Jurado-Chichay and Walker 2001). More generally, the behavior observed at Long Valley and Okataina volcanic systems is similar to that of the Valles/Toledo Caldera (Smith 1979; Spell et al. 1990, 1996), the Yellowstone Caldera (Hildreth 1981, Table 1) and the Timber Moun-

tain/Oasis Valley Caldera (Farmer et al. 1991). It is also common that plutonic rocks associated with volcanism, where they are exposed by erosion, are typically younger than the corresponding volcanic rocks (e.g., Lipman 1988).

Threshold chamber size

Our model predicts that, for large magma chambers (>100 km^3), it is generally difficult if not impossible to produce sufficient overpressure (10–40 MPa) to generate a rhyolite dike capable of causing an eruption. Consequently, once a chamber is sufficiently large, it becomes difficult to drain and magma can accumulate virtually without limit (or at least until a mechanical limit not identified by our model is attained). The question still exists, however, about how to achieve the threshold chamber size. There are several possibilities. Initially, the chamber may be composed of neutrally buoyant (more mafic) magma that is unlikely to erupt. Alternatively, the chamber may initially be fed with a low magma influx, such that the critical chamber overpressure is not reached. Another possibility is that during the early part of chamber growth, the magma in the chamber may have a crystal content sufficiently high that it is uneruptible (cf. Marsh 1988).

Recurrence interval for eruptions and chamber volume

Once a large (>10^2 km^3) silicic magma chamber is established, the theory suggests that the chamber can be drained via dikes and eruptions under only two circumstances. The first is that magma be delivered to the chamber in pulses in which the influx of new magma greatly exceeds the long-term magma supply Q, such that a critical chamber overpressure can be reached. The bigger the chamber, the larger the pulse of new magma that is required for an eruption to occur. As this new magma must first be produced, larger pulses also imply longer times between eruptions. The second circumstance is when the chamber is flattened in the vertical direction (i.e., highly non-spherical), in which case dikes might be generated at the edges of the chamber where the curvature of the chamber walls is high and where stress may be concentrated as new magma enters the chamber. This effect may be enhanced by regional extensional stresses, which will tend to make the formation of dikes most likely at the ends of the chamber aligned with the extension direction.

The requirement for a minimum magma pulse size to generate an eruption leads to a prediction that the eruption interval should be correlated with magma chamber volume (Fig. 6), and the correlation is about the same regardless of whether the wall rocks are responding elastically or in an effectively viscous way. This correlation is difficult to prove in nature because the volume of magma contained in subsurface chambers in regions of active volcanism is not easily estimated and, in addition, a substantial geochronological database is required to establish the recurrence interval. There are enough data for two systems to allow us to begin to evaluate this correlation—the Mono-Inyo Craters of eastern California, and the Okataina system in New Zealand. For the Mono-Inyo system the recurrence interval is in the range of 200 to 700 years for rhyolite eruptions over the past several thousand years (e.g., Metz and Mahood 1985, 1991; Christensen and DePaola 1993; Davies et al. 1994), and the eruption rate is about 0.001 km^3 $year^{-1}$. The recurrence rate is plotted in Fig. 6 using a magma supply equal to the eruption rate. This suggests a chamber volume of about 100 km^3. A higher value for the magma supply would yield a proportionally higher value for the chamber volume. For Okataina, about 80 km^3 of rhyolitic magma has been erupted over the past 21,000 years in nine eruptions (e.g., Nairn 1981). The average interval between eruptions is about 2,200 years and the eruption rate is about 0.004 km^3 $year^{-1}$. The eruption rate and recurrence interval for Okataina correspond to a chamber volume of about 2,000 km^3 (Fig. 6).

Granitic plutons and rhyolitic magma chambers

The model may also be useful for understanding the occurrence and size of large granitic plutons. In order to produce plutons with volumes of order 10^4 km^3, it is necessary to accumulate and store magma for an extended time, as well as to have a magma supply rate that is significantly larger than the rate of internal crystallization. The production of large intrusive bodies, where the magma need not be eruptible, is less demanding than the production of large reservoirs of eruptible rhyolite. If we rearrange Eq. (29), we obtain an expression for the minimum magma influx, Q_{crit}, needed to maintain a magma body with a crystal fraction, f:

$$Q_{crit} = \frac{4\pi qR^2}{\rho(fL + C\Delta T)} = \frac{4.8qV_{ch}^{2/3}}{\rho(fL + C\Delta T)} \tag{31}$$

Hence, the same magma supply can sustain a larger magma body at constant crystal fraction if the magma has higher crystal content. At high crystal contents (f >0.5), the magma apparently cannot erupt because of its high viscosity (Marsh 1988), so the tendency to accumulate rather than erupt magma is stronger than predicted in our model. It is noteworthy in this context that the magma erupted in the largest documented caldera-forming eruption of the Fish Canyon Tuff (>5,000 km^3), which formed the LaGarita caldera in southwest Colorado (Lipman et al. 1997; Bachmann et al. 2003), had a particularly high crystal content (ca. 50% by volume). Granitic batholiths also typically occur in extensional settings (e.g., Atherton 1990), which is consistent with the idea that chamber expansion due to extension will further suppress dike formation. Finally, batholiths are also associated with high crustal heat flow, which is due mostly to efficient

heat transfer within spatially extensive hydrothermal systems (e.g., Taylor 1971; Taylor and Forester 1979; Norton and Knight 1981). In addition to distributing the heat flux from plutons over broad areas, it is well known that hydrothermal circulation leads to fracturing in magma chamber wall rocks. Protracted warming and fracturing will cause the effective viscosity of wall rocks to decline over time, causing them, in turn, to deform in an increasingly viscous way in response to chamber growth (Figs. 4 and 5). A further implication of our model is, thus, that the occurrence and size of large granitic plutons may be a natural consequence of the growth and evolution of a rhyolitic magma chamber that initially supported volcanism.

Our model can explain the development of large magma chambers filled with eruptible, buoyant magma. It does not produce a clear limit on the ultimate size of a magma chamber that can be formed. One limit may be imposed by the magma supply. If the magma supply to a large chamber decreases significantly from the critical value [cf. Eq. (31)], the magma will eventually crystallize sufficiently to become uneruptible (cf. Marsh 1988). We also hypothesize that if large chambers become flattened, eventually the roof may become gravitationally unstable, limiting the ultimate size of calderas. This hypothesis will be investigated in a separate paper. It is noteworthy that, however, our analysis can explain eruption periodicities in the range of 10 years to about 10,000 years (Fig. 6), but cannot explain periodicities of ca. 300,000 to 600,000 years that have been determined for caldera systems in which there have been multiple large CCF eruptions (e.g., Jemez Mountains, New Mexico, the Taupo Volcanic zone, New Zealand, and Yellowstone). As noted above, the buoyancy of a silicic magma layer at the top of a chamber may produce sufficient overpressure to produce dikes if the thickness of the layer approaches 4 km. Consequently, an implication of our results is that with continued growth a chamber initially in the viscous regime could evolve back into the elastic regime. Therefore, the influence of magma buoyancy could act to limit the height, if not the ultimate volume of crystal-poor silicic magma chambers.

Summary and conclusions

Large catastrophic caldera-forming (CCF) eruptions of silicic magma require that large volumes of buoyant magma be stored in shallow magma chambers. The volumes of the largest CCF eruptions, which are in excess of 1,000 km^3, when compared with the typical rates at which magma can be produced in subduction zone and extensional environments (0.001 to 0.01 km^3 $year^{-1}$/volcano), require that magma accumulate and be stored in a chamber over time periods of 10^5 to 10^6 years. Why does buoyant silicic magma get stored rather than erupt at about the same rate it is produced?

We suggest that the evolution of upper crustal silicic magma chambers is controlled by the magma supply to the chamber, the volume of the chamber, and the wall-rock rheology. This conclusion is reached by investigating the pressurization of a spherical chamber of varying size due to influxes of new magma derived from deeper levels and delivered to the magma in pressurized dikes. The deep magma supply is constrained by geological data on the rates of magma generation in the subduction zone and related environments, by the repose times of large eruptions in caldera systems, and by the thermal requirements for maintaining magma in the upper crust at a relatively low degree of crystallinity. Our analysis is based on a nominal long-term average magma supply rate of Q=0.005 km^3 $year^{-1}$, but the conclusions reached vary little if the supply is in the range 0.001 to 0.02 km^3 $year^{-1}$.

Using the equation for a Maxwell viscoelastic solid to describe the response of the wall rock to the expansion of a chamber of radius R_{ch} and volume V_{ch} being fed with new magma at a rate Q, we calculate the maximum magma overpressure (relative to the surrounding wall rocks) that can be generated as a function of Q/V_{ch} and the effective viscosity or flow stress of the wall rocks. The wall rocks are assumed to have either a uniform viscosity (10^{17}–10^{20} Pa s^{-1}), or the power law behavior of wet Westerly granite (Hansen and Carter 1983). The latter gives effective viscosities in the range 10^{21}–10^{17} Pa s^{-1} and flow stress in the range 10^9 to 10^6 Pa for temperatures in the range 300 to 600 °C, and the strain rates (10^{-9}–10^{-14} s^{-1}) that characterize the near field environment of expanding spherical chambers varying in volume from 0.1 to 10^4 km^3.

Small chambers ($V \leq 100$ km^3) with relatively cool wall rocks can be readily pressurized to the critical overpressure (ca. 10–40 MPa) needed to form and propagate rhyolite dikes from the chamber to the surface. The critical overpressure is calculated from the model of Rubin (1995a) and reflects the requirements for sufficiently rapid dike propagation to avoid freezing of the dike tip. It is, therefore, inferred that small chambers with cool wall rocks should generally be drained of magma by eruption at a rate that is similar to the rate that magma is supplied to the chamber from deeper levels. In this regime, eruptions should relieve overpressure, be relatively frequent, and of small volume compared with CCF eruptions. Large chambers ($V \geq 100$ km^3) with warm wall rocks, however, cannot be sufficiently over-pressured to form dikes with the typical long-term supply rate Q. In this regime there is a strong tendency for magma to accumulate in the chamber, for eruptions to be suppressed, and for the chamber to continue to grow in volume as it is fed with new magma. The storage regime can be enhanced by regional extensional stresses, which tend to lower the overpressure attainable near the roof of the chamber, and by increasing temperature in the wall rocks. The storage regime can be overcome by supplying magma to the chamber at a rate that is far above the long-term average value. However, such behavior requires magma to be first accumulated for a time that depends on Q before it is fed into chamber. Large chambers may also produce dikes if they are irregularly shaped (e.g.,

flattened in the vertical direction) such that stresses generated by expansion are concentrated at more strongly curved parts of the chamber wall.

The limitations on magma supply produce additional limitations on the time scale over which magma chambers can be pressurized to produce dikes. This time scale is independent of wall-rock rheology and proportional to V_{ch}/Q. For chamber volumes in the range 10 to 10^4 km^3, this time scale, which equates to the minimum eruption interval, varies from about 10 to 10,000 years. At these time scales, the lag time for pressurization of a pre-existing magma filled crack (cf. McLeod and Tait 1999) is unimportant for determining the frequency of eruptions.

Acknowledgments This manuscript has benefited from a careful review by Steve Sparks and comments by Ross Kerr, Michael Manga, Francis Nimmo, and Tim Druitt. A.M.J. was supported in part by the Miller Institute for Basic Research, University of California, Berkeley, during the completion of this work. The work was also partially supported by NSF-EAR990959 and by a John Simon Guggenheim Foundation Fellowship to D.J.D.

References

Agnon A, Lyakhovsky V (1995) Damage distribution and localization during dyke intrusion. In: Baer, Heimann (eds) Physics and chemistry of dykes. pp 65–78

Anderson AT, Newman S, Williams SN, Druitt TH, Kirius CS, Stolper E (1989) H_2O, CO_2, Cl, and gas in plinian and ash-flow Bishop rhyolite. Geology 17:221–225

Anderson TL (1995) Fracture mechanics: fundamentals and applications. CRC Press, Boca Raton

Atherton MP (1990) The coastal batholith of Peru: the product of rapid recycling of "new crust" formed within a rifted continental margin. Geol J 25:337–349

Bachmann O, Dungan M, Lipman P (2003) The Fish Canyon magma body, Colorado: rejuvenation and eruption of an upper crustal near-solidus batholithic magma chamber upon voluminous mafic underplating. J Petrol (in press)

Bacon CR, Newman S, Stolper E (1992) Water, CO_2, Cl, F in melt inclusions in phenocrysts from 3 Holocene explosive eruptions, Crater Lake, Oregon. Am Mineral 77:1021–1030

Bailey RA (1965) Field and petrographic notes on the Matahina ignimbrite. In: Ewart A (ed) New Zealand volcanology: central volcanic region. NZ Dept Sci Indust Res 80:125–128

Bailey RA, Carr RG (1994) Physical geology and eruptive history of the Matahina ignimbrite, Taupo volcanic zone, North Island, New Zealand. NZ J Geol Geophys 37:319–344

Bailey RA, Dalrymple GB, Lanphere MA (1976) Volcanism, structure, and geochronology of Long Valley caldera, Mono County, California. J Geophys Res 81:725–744

Battaglia M, Roberts C, Segall P (1999) Magma intrusion beneath Long Valley Caldera confirmed by temporal changes in gravity. Science 285:2119–2122

Bibby HM, Caldwell TG, Davey FJ, Webb TH (1995) Geophysical evidence on the structure of the Taupo volcanic zone and its hydrothermal circulation. J Volcanol Geotherm Res 68:29–58

Bienawski ZT (1984) Rock mechanics design in mining and tunneling. Balkema, Boston

Bills BG, Currey DR, Marshall GA (1994) Viscosity estimates for the crust and upper mantle from patterns of lacustrine shoreline deformation in the Eastern Great Basin. J Geophys Res 99:22059–22086

Blake S (1984) Volatile oversaturation during the evolution of silicic magma chambers as an eruption trigger. J Geophys Res 89:8237–8244

Bonafede M, Dragoni M, Quareni F (1986) Displacement and stress fields produced by a center of dilation and by a pressure source in a viscoelastic half-space: application to the study of ground deformation and seismicity at Campi Flegeri, Italy. Geophys J R Astron Soc 87:455–485

Bonin B (1986) Ring complex granites and anorogenic magmatism. North Oxford Academic, Oxford

Bottinga Y, Weill D (1972) The viscosity of magmatic silicate liquids: a model for calculation. Am J Sci 272:438–475

Bower SM, Woods AW (1997) Control of magma volatile content and chamber depth on the mass erupted during explosive volcanic eruptions. J Geophys Res 102:10273–10290

Brace WF, Kohlstedt DL (1980) Limits on lithospheric stress imposed by laboratory experiments. J Geophys Res 85:6248–6252

Bratseva OA, Melekstsev IV, Ponomareva VU, Kirianov VY (1996) The caldera-forming eruption of Ksudach volcano about ca. A.D. 240; The greatest explosive event of our era in Kamchatka, Russia. J Volcanol Geotherm Res 70:49–65

Brown GC, Mussett AE (1981) The inaccessible Earth. Allen and Unwin, London

Bruce PM, Huppert HE (1990) Solidification and melting along dykes by the laminar flow of basaltic magma. In: Ryan MP (ed) Magma transport and storage. Wiley, Chichester, pp 87–101

Cambray FW, Vogel TA, Mills JG Jr (1995) Origin of compositional heterogeneities in tuffs of the Timber Mountain group: the relationship between magma batches and magma transfer and emplacement in an extensional environment. J Geophys Res 100:15793–15805

Carter NL, Tsenn MC (1987) Flow properties of continental lithosphere. Tectonophysics 136:27–63

Cayol V, Dietrich JH, Okamura AT, Miklius A (2000) High magma storage rates before the 1983 eruption of Kilauea, Hawaii. Science 288:2343–2346

Christensen JN, DePaolo DJ (1993) Time scales of large volume silicic magma systems: Sr isotopic systematics of phenocrysts and glass from the Bishop Tuff, Long Valley California. Contrib Mineral Petrol 113:100–114

Christiansen RL (1984) Yellowstone magmatic evolution: Its bearing on understanding large-volume explosive volcanism. In: Explosive volcanism: inception, evolution, and hazards. National Academy Press, Washington, DC, pp 84–95

Cohen AS, O'Nions RK (1993) Melting rates beneath Hawaii; evidence from uranium series isotopes in Recent lavas. Earth Planet Sci Lett 120:169–175

Criss RE, Taylor HP Jr (1983) An $^{18}O/^{16}O$ and D/H study of Tertiary hydrothermal systems in the southern half of the Idaho batholith. Geol Soc Am Bull 94:640–663

Criss RE, Ekren EB, Hardyman RF (1984) Casto Ring Zone: a 4,500 km^2 fossil hydrothermal system in the Challis Volcanic Field, central Idaho. Geology 12:331–334

Crowe BM (1986) Volcanic hazard assessment for disposal of high-level radioactive waste, ch 16. In: Active tectonics: impact on society. National Academy Press, Washington, DC, pp 247–260

Davidson J, DeSilva S (2000) Composite volcanoes. In: Sigurdsson H (ed) Encyclopedia of volcanoes. Academic Press, London, pp 663–682

Davies GR, Halliday AN (1998) Development of the Long Valley rhyolitic magma system: strontium and neodymium isotope evidence from glasses and individual phenocrysts. Geochim Cosmochim Acta 62:3561–3574

Davies GR, Halliday AN, Mahood GA, Hall CM (1994) Isotopic constraints on the production rates, crystallization histories and residence times of pre-caldera silicic magmas, Long Valley, California. Earth Planet Sci Lett 125:17–37

Davies JH, Bickle MJ (1991) A physical model for the volume and composition of melt produced by hydrous fluxing above subduction zones. Phil Trans R Soc Lond A 335:355–364

Davis WJ (1985) Geochemistry and petrology of the Rotoiti and Earthquake Flat pyroclastic deposits. MSc Thesis, Auckland University

DePaolo DJ, Perry FV, Baldridge WS (1992) Crustal versus mantle sources of granitic magmas: a two-parameter model based on Nd isotopic studies. Earth Sci Trans R Soc Edinb 83:439–446
Denlinger RP, Hoblitt RP (1999) Cyclic eruptive behavior of silicic volcanoes. Geology 27:459–462
Dragoni M, Magnanensi C (1989) Displacement and stress produced by a pressurized, spherical magma chamber, surrounded by a viscoelastic shell. Phys Earth Planet Int 56:316–328
Dvorak JJ, Dzurisin D (1997) Volcano geodesy: the search for magma reservoirs and the formation of eruptive vents. Rev Geophys 35:343–384
Farmer GL, Broxton DE, Warren RG, Pickthorn W (1991) Nd, Sr, and O isotopic variations in metaluminous ash-flow tuffs and related volcanic rocks at the Timber Mountain/Oasis Valley Caldera Complex, SW Nevada: implications for the origin and evolution of large-volume silicic magma bodies. Contrib Mineral Petrol 109:53–68
Fialko Y, Simons M, Khazan Y (2001) Finite source modeling of magmatic unrest in Socorro, New Mexico, and Long Valley, California. Geophys J Int 146:181–190
Fournier RO, Pitt AM (1985) The Yellowstone magmatic-hydrothermal system. In: Stone C (ed) Geothermal Resource Council 1985, Symposium on geothermal energy transactions. Geothermal Resource Council, pp 319–327
Green DH (1973) Contrasted melting relations in a pyrolite upper mantle under mid-ocean ridge, stable crust and island arc environments. Tectonophysics 17:285–297
Griffith AA (1920) The phenomena of rupture and flow in solids. Philos Trans R Soc Lond 221:163–197
Hansen FD, Carter NL (1983) Semibrittle creep of dry and wet Westerly granite at 1,000 MPa. 24th US Symposium on Rock Mechanics, Texas A&M, pp 429–447
Hemond C, Hofmann AW, Heusser G, Condomines M, Raczek I, Rhodes JM (1994) U–Th–Ra systematics in Kilauea and Mauna Loa basalts, Hawaii. Chem Geol 116:163–180
Hervig RL, Dunbar N, Westrich HR, Kyle PR (1989) Pre-eruptive water content of rhyolitic magmas as determined by ion microprobe analyses of melt inclusions in phenocrysts. J Volcanol Geotherm Res 36:299–302
Hess KU, Dingwell DB)1996) Viscosities of hydrous leucogranitic melts—a non-Arrhenian model. Am Mineral 81:1297–1300
Hildreth W (1979) The Bishop Tuff: evidence for the origin of compositional zonation in magma chambers. Geol Soc Am Spec Paper 180:43–75
Hildreth W (1981) Gradients in silicic magma chambers: implications for lithospheric magmatism. J Geophys Res 86:10153–10192
Hildreth W, Christiansen RL, O'Neill JR (1984) Catastrophic isotopic modification of rhyolitic magma at times of caldera subsidence, Yellowstone Plateau volcanic field. J Geophys Res 89:8339–8369
Hill DP, Bailey RA, Ryall AS (1985) Active tectonic and magmatic processes beneath Long Valley Caldera, eastern California: an overview. J Geophys Res 90:11111–11120
Huppert HE, Sparks RSJ (1988) The generation of granitic magmas by intrusion of basalt into continental crust. J Petrol 29:599–624
Hutton DHW, Reavy RJ (1992) Strike-slip tectonics and granite petrogenesis. Tectonics 11:960–967
Jellinek AM, Kerr RC (1999) Mixing and compositional stratification produced by natural convection. Part 2. Applications to the differentiation of basaltic and silicic magma chambers, and komatiite lava flows. J Geophys Res 104:7203–7219
Johnson CM (1991) Large scale crust formation and lithosphere modification beneath Middle to Late Cenozoic calderas and volcanic fields, western North America. J Geophys Res 96:13485–13507
Jurado-Chichay Z, Walker GPL (2001a) The intensity and magnitude of the Mangaone Subgroup plinian eruptions from Okataina volcanic center, New Zealand. J Volcanol Geotherm Res 111:219–237
Jurado-Chichay Z, Walker GPL (2001b) The variability of Plinian fall deposits; examples from Okataina volcanic center, New Zealand. J Volcanol Geotherm Res 111:239–263
Kane MF, Mabey DR, Brace RL A (1976) gravity and magnetic investigation of the Long Valley Caldera, Mono county, CA. J Geophys Res 81:754–768
Kerr RC (1994) Melting driven by vigorous compositional convection. J Fluid Mech 280:255–285
Kirby SH (1980) Tectonic stress in the lithosphere: constraints provided by the experimental deformation of rocks. J Geophys Res 85:6353–6363
Kirby SH (1983) Rheology of the lithosphere. Rev Geophys Space Phys 21:1458–1487
Kirby SH (1985) Rock mechanics observations pertinent to the rheology of the continental lithosphere and the localization of strain along shear zones. Tectonophysics 119:1–27
Langbein J, Wilkinson S, Johnston M, Feinberg J, Bilham R (1998) The 1997–98 inflation episode of Long Valley caldera and comparison with the 1989–95 episode. Trans Am Geophys Union (EOS) 79:F963
Lipman PW (1984) The roots of ash flow calderas in western North America: windows into the tops of granitic batholiths. J Geophys Res 89:8801–8841
Lipman PW (1988) Evolution of silicic magma in the upper crust: the mid-Tertiary Latir volcanic field and its cogenetic granite batholith, northern New Mexico, USA. Trans R Soc Edinb Earth Sci 79:265–288
Lipman PW (1995) Declining growth of Mauna Loa during the last 100,000 years: rates of lava accumulation versus gravitational subsidence. In: Rhodes JM, Lockwood JP (eds) Mauna Loa revealed: structure, composition, history, and hazards. Am Geophys Union Geophys Monogr 92:45–80
Lipman PW (2000) Calderas, In: Sigurdsson H (ed) Encyclopedia of volcanoes. Academic Press, London, pp 643–662
Lipman PW, Dungan MA, Bachmann O (1997) Eruption of granophyric granite from a large ash-flow magma chamber: implications for emplacement of the Fish Canyon Tuff and collapse of La Garita caldera, San Juan Mountains, Colorado. Geology 25:915–918
Lister JR, Kerr RC (1991) Fluid–mechanical models of crack propagation and their application to magma transport in dikes. J Geophys Res 96:10049–10077
Lyakhovsky V, Podladchikov Y, Poliakov A (1993) Rheological model of a fractured solid. Tectonophysics 226:187–198
Lyakhovsky V, Reches Z, Weinberger R, Scott TE (1997) Nonlinear elastic behavior of damaged rocks. Geophys J Int 130:157–166
Lyakhovsky V, Ben-Zion Y, Agnon A (1998) Distributed damage, faulting and friction. J Geophys Res 102:27635–27649
Marsh BD (1988) On the crystallinity, probability of occurrence, and rheology of lava and magma. Contrib Mineral Petrol 78:85–98
Marsh BD, Carmichael ISE (1974) Benioff zone magmatism. J Geophys Res 79:1196–1206
McLeod P, Tait S (1999) The growth of dykes from magma chambers. J Volcanol Geotherm Res 92:231–246
McNutt S (2000) Seismic monitoring. In: Sigurdsson H (ed) Encyclopedia of volcanoes. Academic Press, London, pp 1095–1121
Meriaux C, Jaupart C (1995) Simple fluid dynamical models of volcanic rift zones. Earth Planet Sci Lett 136:223–240
Meriaux C, Jaupart C (1998) Dike propagation through an elastic plate. J Geophys Res 103:18295–18314
Meriaux C, Lister JR, Lyakhovsky V, Agnon A (1999) Dyke propagation with distributed damage of the host rock. Earth Planet Sci Lett 165:177–185
Metz JM, Mahood GA (1985) Precursors to the Bishop Tuff eruption: Glass Mountain, Long Valley, California. J Geophys Res 90:11121–11126
Metz JM, Mahood GA (1991) Development of the Long Valley, California, magma chamber recorded in precaldera rhyolite lavas of Glass Mountain. Contrib Mineral Petrol 106:379–397

Michael PJ (1991) Intrusion of basaltic magma into a crystallizing granitic magma chamber: the Cordillera Del Paine Pluton, southern Chile. Contrib Mineral Petrol 108:396–418
Nairn IA (1981) Some studies of the geology, volcanic history and geothermal resources of the Okataina Volcanic Centre, Taupo volcanic zone, New Zealand. PhD Thesis, Victoria University, Wellington
Newhall C, Fink J, Decker B, de la Cruz S, Wagner J-J (1994) Research at Decade volcanoes aimed at disaster prevention. EOS Trans Am Geophys Union 75:340
Newman AV, Dixon TH, Ofoegbu G, Dixon JE (2001) Geodetic and seismic constraints on recent activity at Long Valley Caldera, California: evidence for viscoelastic rheology. J Volcanol Geotherm Res 105:183–206
Norton D, Knight J (1981) Transport phenomena in hydrothermal systems: cooling plutons. Am J Sci 277:937–981
Pallister JS, Hoblitt RP, Reyes AG (1992) A basalt trigger for the 1991 eruptions of Pinatubo volcano? Nature 356:436–428
Palmaesson G, Saemundsson (1974) Iceland in relation to the Mid-Atlantic Ridge. Ann Rev Earth Planet Sci 2:25–50
Petford N, Kerr RC, Lister JR (1993) Dike transport of granitoid magmas. Geology 21:845–848
Petford N, Lister JR, Kerr RC (1994) The ascent of felsic magmas in dykes. Lithos 32:161–168
Perry FV, DePaolo DJ, Baldridge WS (1993) Neodymium isotopic evidence for decreasing crustal contributions to Cenozoic ignimbrites of the western United States: implications for the thermal evolution of the Cordilleran crust. Geol Soc Am Bull 105:872–882
Pollard DD, Segall P (1987) Theoretical displacements and stresses near fractures in rock: with application to faults, joints, veins, dikes, and solution surfaces. In: Atkinson BK (ed) Fracture mechanics of rock. Academic Press, London, pp 277–249
Pritchard ME, Simons M (2002) A satellite geodetic survey of large-scale deformation of volcanic centres in the central Andes. Nature 418:167–169
Punongbayan RS et al. (1991) Lessons learned from a major eruption, Mt. Pinatubo, Philippines. EOS Trans Am Geophys Union 172:545, 552–553, 555
Pyle DM (1998) Forecasting sizes and repose times of future extreme volcanic events. Geology 26:367–370
Reymer A, Schubert G (1984) Phanerozoic addition rates to the continental crust and crustal growth. Tectonics 3:63–77
Ribe NM, Christensen UR (1999) The dynamical origin of Hawaiian volcanism. Earth Planet Sci Lett 171(4):517–531
Richter DH, Eaton JP, Murata KJ, Ault WU, Krivoy HL (1996) Chronological narrative of the 1959–60 eruption of Kilauea volcano, Hawaii. US Geol Surv Prof Pap 537-D
Rubie DC (1983) Reaction enhanced ductility; the role of solid–solid univariant reactions in the deformation of the crust and mantle. Tectonophysics 96:233–261
Rubin AM (1995a) Getting granite dikes out of the source region. J Geophys Res 100:5911–5929
Rubin AM (1995b) Propagation of magma-filled cracks. Annu Rev Earth Planet Sci 23:287–336
Sammis CG, Julian BR (1987) Fracture instabilities accompanying dike intrusion. J Geophys Res 92:2597–2605
Schmitz MD (1995) Geochemical studies of the Rotoiti pyroclastic eruption, Okataina volcanic center, Taupo volcanic zone, North Island, New Zealand. MSc Thesis, Auckland University
Schimozuro D, Kubo N (1983) Volcano spacing and subduction. In: Arc volcanism; physics and tectonics. Proceedings 1981 IAVCEI, pp 141–151
Shaw HR (1972) Viscosities of magmatic silicate liquids: an empirical method of prediction. Am J Sci 272:870–893
Simkin T (1993) Terrestrial volcanism in space and time. Ann Rev Earth Planet Sci 21:427–452
Sims KWW, DePaolo DJ, Murrell MT, Baldridge WS, Goldstein S, Clague D, Jull M (1999) Porosity of the melting zone and variations in solid mantle upwelling rate beneath Hawaii: inferences from ^{238}U–^{230}Th–^{226}Ra and ^{235}U–^{231}Pa. Geochim Cosmochim Acta 63:4119–4138
Smith RL (1979) Ash-flow magmatism. Geol Soc Am Spec Paper 180:5–27
Smith RL, Bailey RA (1968) Resurgent cauldrons. Geol Soc Am Mem 116:613–662
Snyder D, Tait S (1995) Replenishment of magma chambers: comparison of fluid mechanics experiments with field relations. Contrib Mineral Petrol 122:230–240
Snyder D, Tait S (1996) Magma mixing by convective entrainment. Nature 379:529–531
Sparks SR, Sigurdson H, Wilson L (1977) Magma mixing a mechanism for triggering acid explosive eruptions. Nature 267:315–318
Spell TL, Harrison TM, Wolfe JA (1990) $^{40}Ar/^{39}Ar$ dating of the Bandelier Tuff and San Diego Canyon ignimbrites, Jemez mountains, New Mexico: temporal constraints on magmatic evolution. J Volcanol Geotherm Res 43:175–193
Spell TL, McDougall I, Doulgeris A (1996) Cerro Toledo Rhyolite, Jemez volcanic field, New Mexico: $^{40}Ar/^{39}Ar$ geochronology of eruptions between two caldera-forming events. Geol Soc Am Bull 108:1549–1566
Spence DA, Turcotte DL (1985) Magma-driven crack propagation; a mechanism for magma migration through the lithosphere. J Geophys Res 90:575–580
Spera FJ, Crisp JA (1981) Eruption volume, periodicity, and caldera area: relationships and inferences on development of compositional zonation in silicic magma chambers. J Volcanol Geotherm Res 11:169–187
Stormer JC, Whitney JA (1985) Two feldspar and iron–titanium oxide equilibria in silicic magmas and the depth of origin of large volume ash flows. Am Mineral 70:52–64
Tait S, Jaupart C, Vergnoille S (1989) Pressure, gas content and eruption periodicity of a shallow crystallizing magma chamber. Earth Planet Sci Lett 92:107–123
Tatsumi Y, Eggins S (1995) Subduction zone magmatism. Blackwell Science, Oxford
Taylor HP (1971) Oxygen isotope evidence for large-scale interaction between meteoric ground waters and Tertiary granodiorite intrusions, western Cascade range, Oregon. J Geophys Res 76:7855–7874
Taylor HP, Forester RW (1971) Low ^{18}O igneous rocks from the intrusive complexes of Skye, Mull, and Ardnamurchan, western Scotland. J Petrol 12:465–497
Taylor HP, Forester RW (1979) An oxygen and hydrogen isotope study of the Skaergaard intrusion and its country rocks: a description of a 55-m.y.-old fossil hydrothermal system. J Petrol 20:355–419
Wadge G (1980) Output rate of magma from active central volcanoes. Nature 288:253–255
Wallace PJ, Anderson AT, Davis AM (1995) Quantification of pre-eruptive exsolved gas contents in silicic magmas. Nature 377:612–616
Watson S, McKenzie DP (1991) Melt generation by plumes: a study of Hawaiian volcanism. J Petrol 32:501–537
Weinberg RF (1994) Diapiric ascent of magmas through power law crust and mantle. J Geophys Res 99:9543–9560
Wiebe RA (1974) Coexisting intermediate and basic magmas, Ingonish, Cape Breton Island. J Geol 82:74–87
Wiebe RA (1993) Basaltic injections into floored silicic magma chambers. EOS 74:1–3
Wiebe RA (1994) Silicic magmas as traps for basaltic magmas: the Cadillac Mountain Intrusive complex, Mount Desert Island, Maine. J Geol 102:423–437
Wiebe RA (1996) Mafic–silicic layered intrusions: the role of basaltic injections on magmatic processes and the evolution of silicic magma chambers. Trans R Soc Edinb 87:233–242
Wiebe RA, Collins WJ (1998) Depositional features and stratigraphic sections in granitic plutons: implications for the emplacement and crystallization of granitic magma. J Struct Geol 20:1273–1289
Wiebe RA, Blair KD, Hawkins DP, Sabine CP (2002) Mafic injections, in situ hybridization, and crystal accumulation in the

Pyramid Peak granite, California. Geol Soc Am Bull 114:909–920

Wilson CJN, Houghton BF, McWilliams MO, Lanphere MA, Weaver SO, Brigos RM (1995) Volcanic and structural evolution of the Taupo volcanic zone, New Zealand: a review. J Volcanol Geotherm Res 68:1–28

Wilson L, Sparks RSJ, Walker GPL (1980) Explosive volcanic eruptions. IV, The control of magma properties and conduit geometry on eruption column behavior. Geophys J R Astron Soc 63:117–148

Wood CA (1984) Calderas: a planetary perspective. J Geophys Res 89:8391–8406